

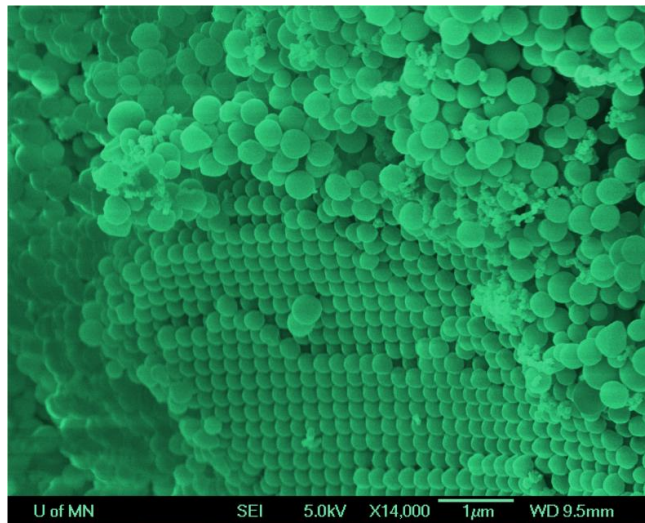
Instituto Politécnico Nacional

Centro de Investigación en Ciencia Aplicada y Tecnología Avanzada

Unidad Legaria

Pigments Based on Colloidal Photonic Crystals

Thesis for obtaining the Ph. D. degree in Advanced Technology by



Carlos Israel Aguirre Vélez

Advisor: Edilso F. Reguera Ruiz (CICATA Legaria IPN, México DF, Mexico)

Advisor: Andreas Stein (University of Minnesota, MN, USA)



INSTITUTO POLITÉCNICO NACIONAL

SECRETARÍA DE INVESTIGACIÓN Y POSGRADO

CARTA CESIÓN DE DERECHOS

En la Ciudad de México D.F. el día 10 del mes Diciembre del año 2010, el (la) que suscribe Carlos Israel Aguirre Vélez alumno (a) del Programa de Doctorado en Tecnología Avanzada con número de registro A080489, adscrito a CICATA Legaria, manifiesta que es autor (a) intelectual del presente trabajo de Tesis bajo la dirección de Dr. Edilso Francisco Reguera Ruiz y Dr. Andreas Stein y cede los derechos del trabajo intitulado "Pigmentos basados en cristales fotónicos coloidales" (Pigments Based on Colloidal Photonic Crystals), al Instituto Politécnico Nacional para su difusión, con fines académicos y de investigación.

Los usuarios de la información no deben reproducir el contenido textual, gráficas o datos del trabajo sin el permiso expreso del autor y/o director del trabajo. Este puede ser obtenido escribiendo a la siguiente dirección c_aguirre_velez@hotmail.com. Si el permiso se otorga, el usuario deberá dar el agradecimiento correspondiente y citar la fuente del mismo.

Carlos Israel Aguirre Vélez

Nombre y firma



INSTITUTO POLITÉCNICO NACIONAL
SECRETARÍA DE INVESTIGACIÓN Y POSGRADO

ACTA DE REVISIÓN DE TESIS

En la Ciudad de México D.F. siendo las 13 horas del día 9 del mes de Diciembre del 2010 se reunieron los miembros de la Comisión Revisora de la Tesis, designada por el Colegio de Profesores de Estudios de Posgrado e Investigación de CICATA Legaria para examinar la tesis titulada:

"Pigmentos basados en cristales fotónicos coloidales" (Pigments based on colloidal photonic crystals)

Presentada por el alumno:

AGUIRRE VELEZ CARLOS ISRAEL
Apellido paterno Apellido materno Nombre(s)

Con registro:

A	0	8	0	4	8	9
---	---	---	---	---	---	---

aspirante de:

DOCTOR EN TECNOLOGIA AVANZADA

Después de intercambiar opiniones los miembros de la Comisión manifestaron **APROBAR LA TESIS**, en virtud de que satisface los requisitos señalados por las disposiciones reglamentarias vigentes.

LA COMISIÓN REVISORA

Directores de tesis

Dr. Edilso Francisco Reguera Ruiz

Dr. Andreas Stein

Dr. Ernesto Marín Moares

Dr. Miguel Ángel Aguilar Frutis

Dr. José Antonio Calderón Arenas

PRESIDENTE DEL COLEGIO DE PROFESORES

Dr. José Antonio Irán Díaz Cóngora

Thesis dissertation in México City January 14th 2011, in the presence of the judge:

Tesis defendida en México D.F. 14 de Enero 2011 ante el jurado:

Dr. José Antonio Calderón Arenas (presidente)

Dr. Ernesto Marín Moares (secretario)

Dr. Edilso F. Reguera Ruiz (primer vocal)

Dr. Andreas Stein (segundo vocal)

Dr. Miguel Ángel Aguilar Frutis (tercer vocal)

Dr. José Guzmán Mendoza (suplente)

Para mis familiares:

Guadalupet, Porfirio†, Graciela†, Nadia, Rocio y Roberto

Para los pilares de mi vida:

Sonia Maricruz, Karla Sofia y Jana Carolina

Acknowledges

I want to thank to everyone who support academically, emotionally and economically this work.

Firstly I want to thank to my advisors Edilso Reguera and Andreas Stein their trust in me, because I did not any previous experience in materials science and they give me the opportunity to get into the world chemistry.

I learn so much with my partners in CICATA Legaria LAB: Manuel, Marlene, Claudia, Carmen, Blanca, Cecilia, Alvaro, Elizabeth, Alejandro, Arianee, Omar, Cristina, Adela, Javier, Juan, Sofía; and my partners in University of Minnesota: Nick 1, Nick 2, Fan, Melissa, Won, Davis, Ahn, Yuqiang

For the great support of CICATA *Legaria IPN PTA* staff members and *CICATA Legaria IPN LAB*: Lety, Pablo, Laura, Mónica, Alicia, Alfonso y “Cuco”.

And finally the economical support of CONACyT Mexico and National Polytechnic Institute (IPN).

Contents

Preface	9
1. State of the art	13
1.1. Pigments and Structural Color.....	14
1.2. Overview of Photonic Crystals.....	20
1.3. Optical Properties of Colloidal Photonic Crystals.....	25
1.4. Tunable Color of Opals and Inverse Opal Photonic Crystals.....	30
2. Experimental	54
2.1 Synthesis of Spheres.....	56
2.2 Assembly of Opal Structure.....	57
2.3 Mixtures of Carbon with Opaline Powders.....	58
2.4 Preparation of Photonic Paint	59
2.5 Instruments.....	60
3. Results and discussion	62
3.1 Colloidal Photonic Pigments with Low- Angle-Dependence.....	63
3.2 Elements for modeling color effect for Colloidal Photonic Pigments with Low- Angle-Dependence.....	75
4. Conclusions and Further work	83
5. References	87
Appendix 1.	95
Appendix 2.....	109

Abstract

Colloidal photonic crystals are periodic structures which reflect certain wavelengths and transmit other ones. This kind of structure exhibits coloration due to diffraction and interference of light. The color based on optical phenomena is called structural color; it is the same mechanism by which butterflies and other animals show color. Structural color of colloidal photonic crystals (synthetic opals) is used for the fabrication of a novel pigment made of a mixture of polymer and carbon, uncommon materials in the pigment industry. This colored powder does not show iridescence to the naked eye, its fabrication it is very easy and can be considered as a pigment option complementing traditional organic and inorganic pigments. This work is about synthesis, characterization and modeling of novel photonic pigments.

Resumen

Los cristales fotónicos coloidales son estructuras periódicas que reflejan ciertas longitudes de onda y dejan pasar otras. Esta clase de estructuras exhiben coloración debido a difracción e interferencia de la luz. El color basado en fenómenos ópticos es conocido como color estructural; es el mismo mecanismo usado por mariposas y otros animales para mostrar color. El color estructural de los cristales fotónicos coloidales (u ópalos sintéticos) es utilizado para la fabricación de un nuevo pigmento hecho de polímero y carbón, materiales no comunes en la industria de pigmentos. Este polvo colorido no muestra iridiscencia al ojo, su fabricación es sencilla y puede considerarse como una opción ante los pigmentos tradiciones orgánicos e inorgánicos. Este trabajo trata acerca de la síntesis, caracterización y modelado de nuevos pigmentos fotónicos.

Preface

Color is important for the human race and most animals: it is a medium to distinguish differences, to classify objects, to indicate changes, to catch at a glance; it is even used just as a symbol or icon.

Color is not just painted stuff. It is a process which involves four elements: 1) a light source, 2) coloring materials applied to objects, 3) the color system of the eye and 4) the way of signifying of color in the brain (psychology). In this work we refer only to the second element in the figure of pigments.

Most pigments are based on absorption of certain wavelengths in the visible range by different mechanisms involving the molecular structure. Usually, in the pigment industry, each color is achieved at least with one chemical compound; therefore different colors originate from different compounds. But some pigments are based on physical effects: diffraction, interference, scattering, iridescence. Colors derived from physical mechanisms are called structural colors.

Structural colors are manufactured based on periodic structures; the way in which several animal species exhibit color in their bodies, wings, feathers, and scales, not by chemical compounds but through physical structures. Another material that shows structural colors is the opal gemstone. This material is essentially composed of little spheres made of silica in periodic arrays.

One advantage of structural colors is that they are not bleached by UV radiation, but a disadvantage -for some applications- is the iridescence or change of color depending on the viewing angle.

Structural color is also exhibited by other kinds of structures called photonic crystals.

Photonic crystals are periodic structures that can be thought of as a particular filter over a range of certain wavelengths. When an incident white light beam interacts with this kind of material, it transmits a range of wavelengths and reflects other ones.

The material shows one color observed by reflection and shows another color observed by transmission. Colloidal photonic crystals (or synthetic opals) exhibit iridescence when they are viewed at from different angles similarly to an opal gemstone.

The idea of having pigments based on structural color without iridescence sounds interesting because they could be an alternative for some toxic inorganic pigments, and for organic pigments some of which are unstable under UV radiation. Pigments that do not depend on properties of chemical bonding just from refractive index and geometrical parameters, could be applied where other pigments are weak in their color properties.

Although opal structures have been used in different configurations to fabricate new photonic materials, and the optical properties have been studied intensively, new opportunities remain for developing applications.

This work is about a novel application based on colloidal photonic crystals, different to those that have been previously reported or registered as patents and that could be potentially carried to industry. We have developed colored powders, which we refer to as “photonic pigments”, with the following features:

- a) Ease of use in the synthesis process
- b) The use of only a small number of chemical compounds for obtaining many different colors
- c) A uniform appearance of color without iridescence to the naked eye
- d) A non- bleaching effect on color
- e) The possibility having pigments made with environmentally friendly materials

Independent of the potential commercial advantages, the colored powder itself is important because it is the first pigment using structural color without iridescence to the naked eye. Moreover, it is interesting how a mixture of white and black powders results in colored powders, without chemical reactions in the process.

Using these photonic pigments it was possible to fabricate a basic paint that was applied to some kind of surfaces. This is exciting because it opens up the possibility for developing commercial paints made with materials uncommon in the paint industry.

The main differences of these photonic pigments compared to patented ones is the incorporation of carbon that makes a matte appearance, whereas patented pigments are iridescent. Another big difference has to do with the fabrication process; the photonic pigments we developed do not need a careful depositing over a prepared surface.

Theoretically it is important to understand how photonic pigments work. The operating principles of these pigments involve different optical effects whose combination has not been considered before.

The research was inspired by experimental observations about how opaline powders, when spread over a large dark surface, look colored without iridescence under natural white light. This effect can be seen for different kinds of dark surfaces, independent of their nature. This observation leads us to believe that chemical bonding could not be involved in the color effect.

The question that guided our work was: why do dark surfaces enhance the color of opaline powder? We made a hypothesis: **if any dark surface enhances the color of colloidal photonic crystals powders, carbon can work in a similar way.**

The general objective of this work is: **the study of mixtures of colloidal photonic crystals with carbon in order to make pigments that produce a coloration based on structural color.**

The specific objectives are:

- a) The synthesis and characterization of samples (colloidal photonic crystals)
- b) A theoretical approach for modeling the effect of a dark surface behind of colloidal photonic crystals
- c) The possible application of this new pigment in a paint

This work establishes in chapter 1 (the state of the art), the theoretical background for understanding the of content: structural color, photonic crystals and particularly the optical features of colloidal photonic crystals. In the same section a review of materials capable of changing color under external stimuli, based on opals and inverse opals, is shown as interesting ways to achieve variable and reversible coloration.

In the experimental section (chapter 2) the process of synthesis used for spheres is described, the method for assembling the spheres, the mixtures of carbon with opaline powders, the preparation of paint and the instruments used for characterization.

The results of our experiments are shown in chapter 3: spectra, SEM images, visual images and graphics provide supporting information. A theoretical analysis of the effects involved in the color effect is also discussed in this section. Finally, in chapter 4 some further work and conclusions with comments and works referenced are provided.

The main ideas discussed here have been reported in the following published papers (appendix 1 and 2):

- Aguirre C. I.; Reguera E.; Stein A. Tunable color by opals and inverse opal photonic crystals *Functional Advanced Materials* **2010**, 20, 2565
- Aguirre C. I.; Reguera E.; Stein A. Colloidal photonic crystals pigments with low angle dependence, *Applied Materials & Interfaces* **2010**, 2, 3257

Part of this work participated in:

- The Ninth International Conference on Photonic and Electromagnetic Crystal Structures (PECS-IX 2010), 26-30 September 2010 in Granada Spain
- Advanced Technology Symposium 5 (2010 June) Mexico City

1. STATE OF THE ART

1. state of the Art

1.1. Pigments and Structural Color

1.1.1 Pigments

There are several mechanism of color; Nassau has discussed fifteen causes of color in his classic book. ^[1] They can be divided in two major groups, based on chemical phenomena and on optical phenomena.

Pigments and dyes are coloring materials based on chemical phenomena. Pigments are insoluble solids that not are affected physically or chemically by the substrate in which they are incorporated and dyes are coloring substances that have an affinity for the substrate to which they are applied.

There are several uses for pigments in a wide variety of materials. Usually, each color is made by one or several compounds and their applications determine the kind of pigment to be chosen.

Pigments can be classified by their origin (natural or synthetic), by chemical class (organic or inorganic), by their color (white, black and colored) or by their special effects (pearlescent or nacreous, interference, metallic, fluorescent, phosphorescent). Inorganic pigments can be sub-classified as oxides, sulfides, oxide hydroxides, silicates, sulfates and carbonates. Inorganic pigments can be divided into two groups: azo and polycyclic pigments.

The mechanisms involved in the interaction between light and pigments are straightforward. When a photon enters into a pigmented coating three processes can occur:

- The photon collides with the pigmented particle and is absorbed
- The photon collides with the pigmented particle and is scattered
- The photon passes through the coating without collision and is scattered and/or absorbed by the substrate

The chemical mechanisms for obtaining color are based on quantum mechanics: some involve ligand field effects (hybrid orbitals in transition metals compounds), some molecular orbital effects (HOMO-LUMO transitions in organic compounds), some charge transfer effects (in some metallic oxides), and some band gap effects (in semiconductors). Despite its origin, organic or inorganic compound, in the end the color in pigments is due to the absorption of certain wavelengths between two energy levels in the wavelength range of 400 to 700 nm.

The optical properties of pigments are essentially based on scattering and absorbing properties. White pigments have very little absorbing power in comparison to their scattering power. Black pigments have very little scattering power relative to their absorbing power. Colored pigments selectively absorb and scatter light as a function of wavelength.

1.1.2 Structural color

Coloration can be obtained by an optical phenomenon called structural color.

Structural coloration involves the selective reflection of incident light when it interacts with physical structures in spatial variations comparable to the wavelength of light. Structural color can be developed by thin film interference (in soap bubbles), multiple interference (in multilayer dielectric filters), diffraction gratings (on a CD surface), polarization inside birefringent materials (for example, calcite) and photonic crystals.

Figure 1 shows the geometry for a constructive interference of a single layer. The combination of Bragg's law and Snell's laws gives us an equation that describes the condition by which certain wavelengths can be reflected constructively. ^[2] Considering Fig. 1, it is possible to construct the difference in path length (G) between rays R_2 and R_1 that interact with two media of different refractive indices.

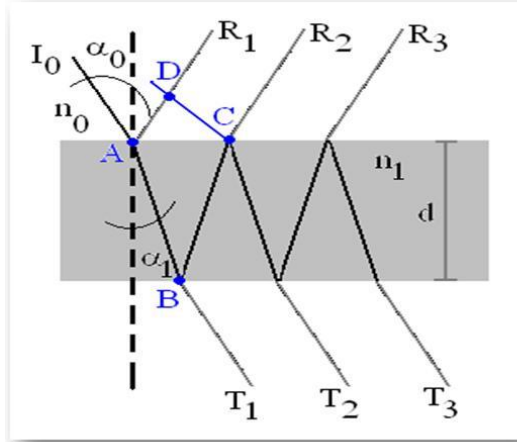


Figure 1. Scheme of constructive interference by single layer.

By applying the law of reflection, we see that $AB = BC$, and then:

$$G = 2n_1 \overline{AB} - n_0 \overline{AD} \quad (1)$$

$$G = 2n_1 \left(\frac{d}{\cos \alpha_1} \right) - 2n_0 \left[\left(\frac{d}{\cos \alpha_1} \right) \frac{n_0}{n_1} \sin^2 \alpha_0 \right] \quad (2)$$

Where n_0 and n_1 are the refractive index involves in two media, α_0 is the incidence angle, α_1 is the refracted angle and d is the width of the layer. Using Snell's law

$$n_0 \sin \alpha_0 = n_1 \sin \alpha_1 \quad (3)$$

and trigonometric relationships, we may substitute Eq. 3 into Eq. 2:

$$G = 2n_1 d \sqrt{1 - \frac{n_0^2}{n_1^2} \sin^2 \alpha_0} \quad (4)$$

The phase difference between the two paths is:

$$\delta = \frac{2\pi}{\lambda} G \quad (5)$$

For constructive interference, $\delta = 2m\pi$ and then $m\lambda = G$, where m is the order of reflection for which interference occurs and λ is the light wavelength.

$$m\lambda = 2d\sqrt{n^2 - n_0^2 \sin^2 \alpha} \quad (6)$$

The analogy with Bragg's law is direct because the reflective optical surfaces play the role of atomic emitters in the lattice.

Iridescence itself has been applied to pigments. With these kinds of pigments the effect is achieved by tiny flakes -of mica and alumina- which interfere with incident white light that produces colorful sparks; there are several arrays to create different pigments with this effect.^[3]

The key in the relationship between color and optical effects is the contrast of refractive index media. For example, white is the result of scattering elements inside other media; chromatic dispersion is an effect of refractive index as a function of wavelength and wavelength filters use a stack of dielectrics in order to reject certain colors.

Probably the most beautiful application of structural color is in biological systems. The active mechanism is usually multiple layered structures composed of keratin, chitin, calcium carbonate and so on, frequently backed by a dark layer of melanin which intensifies the color by absorbing the non-reflected light.

Colors in several living creatures such as beetles, fishes, butterflies, moths, birds, peacocks shells, even in some plants have been intensely studied.^[4, 5, 6] Images produced by a scanning electron microscope have made possible the observation of periodic structures of feathers, skin, leaves, and to model their optical behavior. Studies regarding the photonic structure of bugs are constantly reported in scientific literature.

1.1.3 Characterization and modeling of pigments

Modern testing of coloring materials has been able to establish a relation between color stimuli and fundamental physical quantities. ^[7] The characterization of a pigment can be analyzed at different theoretical levels, from a spectrum to refractive index and geometry from individual particles. The most common approaches to characterizing and modeling interactions between light and pigment particles, from simple spectra to electromagnetic fields modes in particles, are:

- Colorimetry
- Kubelka - Munk theory
- Multiple scattering theory
- Mie solution

When we talk technically about color we refer to it through chromatic coordinates, which relates perceived color quality to the reflection spectrum and the color stimulus. The Commission Internationale de l'Eclairage (CIE) accepts different color spaces, one of which is $L^*a^*b^*$ (based on nonlinearly compressed CIE XYZ color space). The creation of international standards has made it possible to state unambiguously what requirements pigments have to meet, and test methods. Several standards of measurement have been established for testing pigments and have been globally accepted.

For the characterization of pigments with optical effects it is difficult to determine defined parameters because there are different variables involved. Vukusic and Stavenga have reviewed different methods, some based on the Bidirectional Reflectance Distribution Function (BRDF) using gonioreflectometers, for measuring structural color in biological systems.^[8]

Kubelka - Munk's (K-M) theory, was originally derived in 1931 by P. Kubelka and F. Munk ^[9] in order to predict the optical properties of any given material. Such theory is important in industrial application where the color and appearance of the final product is relevant. The K-M theory is based on the model of two flux scattered light when incident light interacts with a sample: reflected (backward direction) and transmitted (forward

direction). Internal reflections inside the sample follow a recursive interaction which requires differential equations to describe the variations of light fluxes as they penetrate into the material. The solution requires the coating thickness, the scattering coefficient ($S(\lambda)$), and the absorption coefficient ($K(\lambda)$). These values can be calculated based on a spectrum. The K-M restrictions, because some assumptions were imposed during its derivation, are useful and sufficient for certain applications.

Scattering by random media (composed of many particles in random positions) is common when incident radiation interacts many times with particles after reaching the surface. In multiple scattering theory, the randomness of the interactions tends to be averaged out by the large number of scattering events, so the final path of the radiation appears to be a distribution of intensity. Multiple scattering is very complicated to calculate from Maxwell equations, and for this reason it is easier to think of it as a diffusion process. The main parameter is the mean free path, which relates scattering interactions among two particles with transmission and the thickness of sample.

In 1908, Gustav Mie published a study about optics of turbid media, particularly of colloidal metal, where he solved an analytical problem for the scattering of an electromagnetic wave by a homogeneous dielectric sphere. Mie's solution relates the refractive index (complex if the material has absorption), the particle size and geometry of a particle with the reradiated light from the scatters. Spheres and some other systems of symmetric particles have been studied using many numerical methods. For applications of scattering using irregular particles it is a challenge to model the scattering while taking into account the inner vibrational modes of the electromagnetic field.

Each approach gives us information at a certain level. Depending on applications some parameters can be useful.

1.2 Overview of Photonic Crystals

One way to control the optical properties of materials is to construct an array of elements capable of modifying the path of light in a similar way to electrons that can modify their behavior in an electrostatic potential.

A photonic crystal is an ordered dielectric structure having spatially periodic different refractive indices modulated alternate materials with lattices comparable to the wavelength of the electromagnetic radiation in order to generate a band gap in photonic regime. ^[10] There are periodic arrays in one, two or three dimensions (**Fig. 2**). The quarter wave stack, used for dielectric mirrors, can be thought of as a 1D photonic crystal.

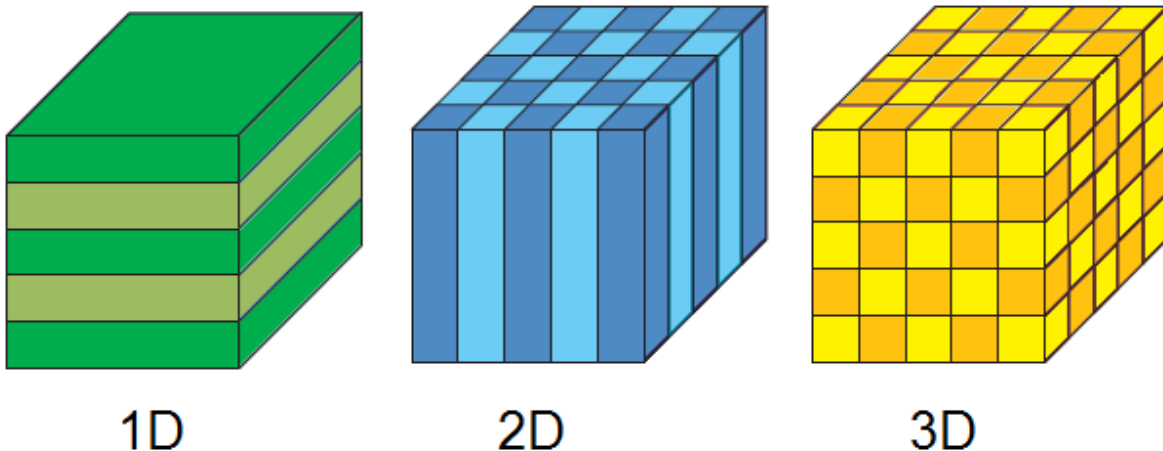


Figure 2. Schematic arrays of 1D, 2D and 3D periodical arrays of dielectric materials.

Scheme was taken from Joannopoulos [10].

When light interacts with a periodic structure there is a coherent superposition of the partial scattering of the wave at each element, permitting some frequencies to propagate through the structure and only in certain directions while waves with other frequencies are blocked. The observed effect is that light having such blocked frequencies will be strongly reflected by the structure. The range of blocked or forbidden frequencies is called the band gap of reflection band, or Photonic Band Gap (PBG).

A crystal with a complete PBG will obviously be an omnidirectional reflector for a specific wavelength. This effect is only possible to achieve by 3D arrays.

Three factors define the PBG of a photonic crystal: 1) the refractive index contrast between diffracting elements and its surroundings, 2) the crystal symmetry and 3) the lattice constant (spatial period of the modulation).

In order to know the behavior of light inside a three-dimensional periodic structure, it is necessary to solve Maxwell's equations without sources, and their combination results in the following wave equation.

$$\nabla \times \left[\frac{1}{\varepsilon(\mathbf{r})} \nabla \times \right] \mathbf{H}(\mathbf{r}) = \left(\frac{c^2}{\omega^2} \right) \mathbf{H}(\mathbf{r}) \quad (7)$$

This is an eigenvalue equation with eigenvectors $\mathbf{H}(\mathbf{r})$ and eigenvalues $\left(\frac{c^2}{\omega^2} \right)$. The operator acting on $\mathbf{H}(\mathbf{r})$ is Hermitian, so the eigenvalues are real and the eigenvectors form an orthogonal set of solutions. Only a few geometries can be analyzed using exact analytical methods. For most photonic crystals with practical importance, numerical simulations are required to know the behavior of light interacting with them.

There are several theoretical approaches to calculating the interaction of light with photonic crystals, such as the plane wave expansion method, the finite-difference time domain (FDTD), and others. ^[11] The solutions are eigenfrequencies, which are plotted as a function of wave vectors tracing the edges in a dispersion diagram. The

Fig. 3 shows two examples for 3D photonic structures: Yablonovite and woodpile.

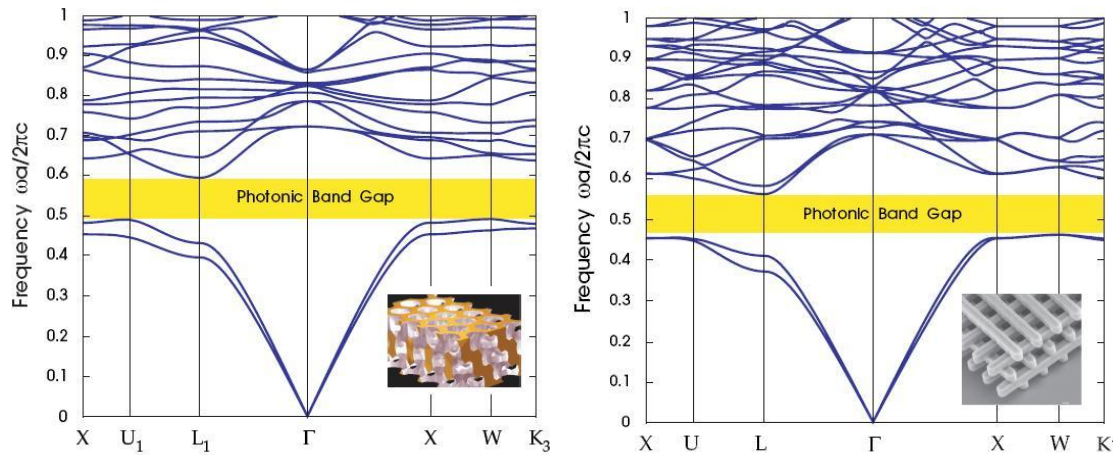


Figure 3. The photonic band structure for two 3D photonic crystals: a) Yablonovite and b) woodpile.

Yellow areas indicate the complete PBG. Images were taken from Joannopoulos [10].

Analogies between the semiconductors and photonic crystals allow the use of same tools of solid state physics for analysis of photonic structures, such as Bloch waves, reciprocal space, Brillouin zone, dispersion diagrams, band structure, etc.

Considering the periodicity of crystal structures in space, it is “natural” to think of Fourier transformation. Fourier analysis decomposes the periodic spatial arrangement of the crystal into its spatial frequency components. Describing a crystal in this way is useful because the space of spatial frequencies, or k -space, is also the space used to characterize the electromagnetic waves according to their wave vector k . We identify the set \mathbf{g} as the fundamental vectors of a lattice in k -space, which are called the reciprocal lattice or reciprocal space.

An array of elements in real space forming a lattice can be transform in its corresponding reciprocal lattice. The details on how to construct of these shapes can be found in any standard text on solid state physics.^[12] The minimum cell that can be considered for analyzing for the photonic behavior in frequencies is known as Wigner-Seitz cell, or first Brillouin zone (BZ).

Each point $[hkl]$ in the reciprocal lattice corresponds to a set of lattice planes in the real space lattice (hkl) . The direction of the reciprocal lattice vector corresponds to the normal of the real space planes, and the magnitude of the reciprocal lattice vector is equal to the reciprocal interplanar spacing of real space planes.

For example, the solid that represents the Brillouin zone, corresponding to a face-centered cubic (fcc) lattice of elements, is a rhombic dodecahedron composed of 12 rhombuses oriented such that each square face intersects with real axes (**Fig. 4**). There are certain symmetric points: the Γ point stays at the center of the solid, while the other points (L, W, U, K and X) stay on its surface. The intersection point with the $[100]$ direction is called X; the line Γ —X is called Δ . The intersection point with the $[110]$ direction is called K; the line Γ —K is called Σ . The intersection point with the $[111]$ direction is called L; the line Γ —L is called Λ .

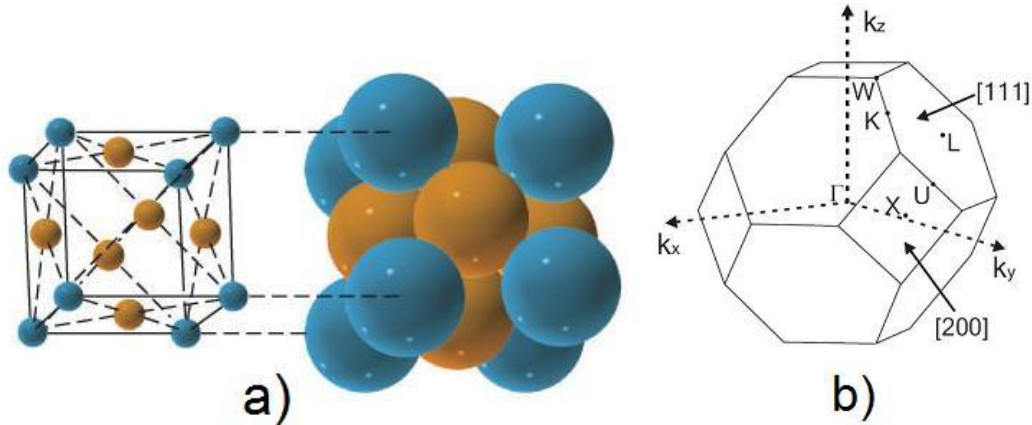


Figure 4. Face centered cubic (fcc) lattice: a) in real space b) in k-space (Brillouin Zone). Image (a) was taken from http://www.nyu.edu/classes/tuckerman/honors.chem/lectures/lecture_20/node2.html

Making the Fourier series analysis of a periodic structure, each face of BZ corresponds to a different term in that series. The directions perpendicular to each face correspond to reciprocal lattice vectors. These vectors contain information about the periodicities of the structure. The shortest vectors correspond to leading terms in the Fourier expansion, and the longer vectors correspond to higher harmonics. The BZ can be used as the basis for both a quick estimate of reflected colors and a complete detailed numerical calculation of band gap.

The distance of each point on the surface of the BZ from the center of the BZ is directly proportional to the frequency in the center of the PBG. Thus, the vertices (which are the furthest out) represent high frequencies (shorter wavelengths), and the center of faces (which are closer in) represents low frequencies (longer wavelengths). This variation is the ultimate origin of iridescence in the visible range of electromagnetic spectrum.

The width of each gap is related to the magnitude of the corresponding Fourier component. The magnitudes of the Fourier components depend on the local structure but also on the refractive index contrast (the ratio of the refractive index of periodical materials). As this contrast increases, the gaps become wider; if the gaps are sufficiently wide, they can then overlap. If several gaps overlap, a complete PBG is formed; that is, a range of wavelengths can be reflected from any direction and any polarization.

The dispersion function demonstrates how frequencies (energy) vary as a function of wave vector (direction). In a periodic system, for a particular choice of \mathbf{k} , a discrete set of eigenfrequencies serve as solutions of the eigenvalue equation. The discrete bands are enumerated in order of increasing frequency. All solutions with the common counting number are collectively called n_{th} photonic band; for this reason the dispersion diagram is called a band diagram.

It is important to note that in the horizontal axes in the band diagram, the directions, given by wave vectors, are put in straight lines, oriented in different directions in reciprocal space.

The band structure of photonic crystals can be used to derive the boundary conditions for the electromagnetic field at the interface of a finite crystal in order to determine transmission and diffraction properties.

For example, in reciprocal space, the parallel components of the wave-vector must be conserved. The energy must be conserved. Light refraction is determined by conservation of the component of the light wave-vector parallel to the interface between the two media, and also by the dispersion surface. In a photonic crystal, light refraction follows a more complicated behavior. The dispersion surface adopts very complicated shapes in these materials due to the dispersion relation, which is known as anomalous refraction effect.

In a material with a complete PBG, light with a specific wavelength cannot propagate in any direction. For frequencies in the visible range, it has not yet been possible to obtain a complete PBG but instead only structures with an incomplete PBG or pseudo PBG, due to the limited options of materials with high refractive index that also do not absorb visible light. A pseudo PBG in the visible range results in materials whose colors vary with the viewing angle.

1.3 Optical Properties of Colloidal Photonic Crystals

Since photonic crystals were proposed in 1987 by Yablonovitch ^[13] for the inhibition of spontaneous emission, and by John for photon localization ^[14], there have been many efforts to fabricate photonic crystals with a complete band gap, mainly in 3D structures: micromachining, layer by layer lithography, autocloning techniques, electro-photo-chemical etching of silicon, holographic lithography, among others. ^[15] The main disadvantage of these top-down approaches is the complex experimental requirements for laboratories, which implies higher costs for massive applications.

Chemical approaches (bottom-up) have been an alternative route to obtain three-dimensional structures for photonic purposes. One of the most important architectures is based on natural opal gemstones.

Synthetic opals, or colloidal photonic crystals are arrays of spheres whose diameter sizes are comparable to the wavelength of visible light, formed through a colloidal self-assembly process. The high monodispersity of the spheres defines the minimum free energy configuration to make the crystalline face-centered-cubic structure. **(Fig. 5)** The microsphere arrays show bright visible iridescence due to Bragg reflections from the crystallographic planes of the structure.

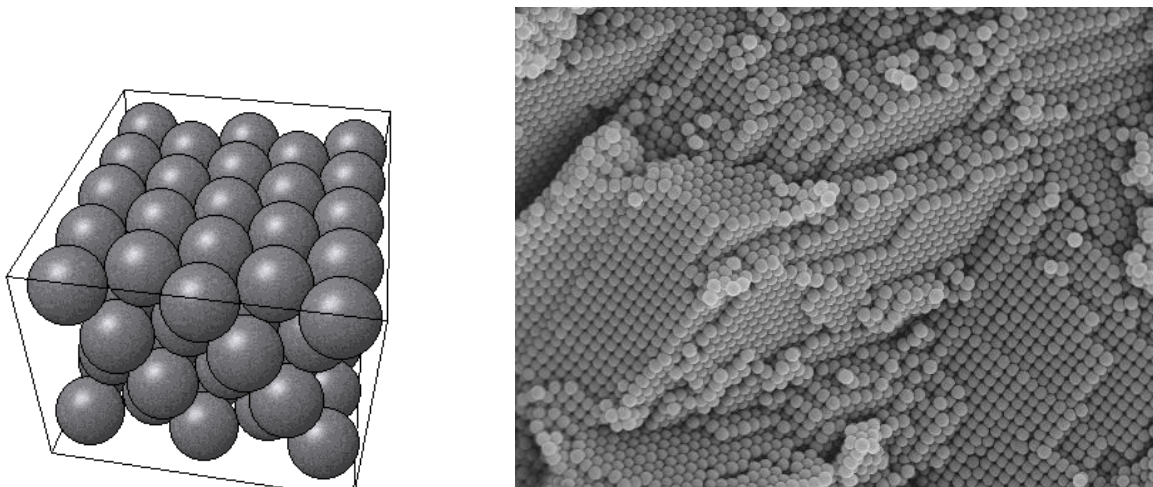


Figure 5. Synthetic opal or colloidal photonic crystal: a) scheme of fcc array of spheres, b) SEM image of synthetic opal growth in the laboratory.

The idea of using opal arrays as photonic crystal systems comes from nineties, in 1995 when Astratov *et al.* reported the use of silica opals ^[16]. After that breakthrough, other materials have been studied: titania (TiO₂), polystyrene (PS) and poly(methylmethacrylate) (PMMA), which are among the most common materials used, although other polymers, polymer composites and several oxide opals have been reported, too.

The optical performances of artificial opals is limited by the relatively low refractive index of the spheres; due to the ratio of the refractive index value of available spheres materials, it is not possible to reach a complete PBG in fcc arrays; in order to form a complete PBG it is necessary a ratio of the refractive index at least of 2. ^[17]

Although opal structures don't have a complete PBG, they have been used as: three dimensional photonic crystals for photonic pigments with iridescence ^[18, 19, 20], core-shell structures ^[21], elements of composites for tuning colors under different stimuli ^[22], and templates for inverse structures.

The concept of an "inverse opal" means that we invert the systems, so instead of a sphere of dielectrics and air between voids, we have a dielectric in the voids and air spheres (**Fig. 6**). The route for preparing inverse opals begins with an opal made of polymer spheres, which is infiltrated later with a metallic precursor in order to synthesize metallic oxides, and after the infiltrated structure is carried to a thermal process in which the precursor forms the oxide and the polymeric spheres are burned.

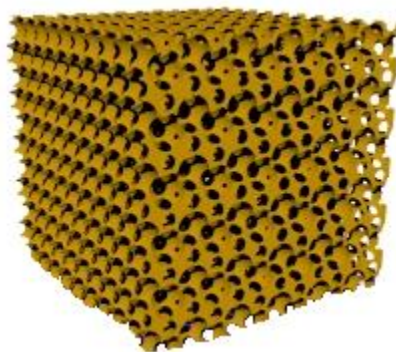


Figure 6. Inverse opal structure.

Stein and coworkers reported the synthesis and optical characterization of inverse opals of metallic oxides by the infiltration of different solvents. ^[23]

The first optical analysis that we can make for an opal is using Bragg's law in order to know the reflectance peaks in the spectrum.

For opals and inverse opals the refractive index n can be taken as an average of the refractive indices of the spheres and the interstitial space for opals, or of spherical voids and solid walls, for inverse opals.

$$n_{avg} = \phi n_{spheres} + (1 - \phi) n_{background} \quad (8)$$

Here ϕ is the solid fraction of the material. The distance d can be taken as d_{hkl} , the spacing between close-packed planes of voids, which is:

$$d_{hkl} = \frac{D\sqrt{2}}{\sqrt{h^2+k^2+l^2}} \quad (9)$$

Here D is the pore spacing, and h, k and l are the indices of Miller planes. For the (111)

plane, $d_{hkl} = D\sqrt{\frac{2}{3}}$. If $n_0 \approx 1$, we then obtain for the first order ($m = 1$):

$$\lambda = 1.633\sqrt{n_{avg}^2 - \sin^2\alpha} \quad (10)$$

Although this expression does not take into account several other details, such as the coupling of incident and diffracted waves due to strong scattering,^[24] it is useful and predicts the reflection peak maxima (λ) that are in good agreement with experimental observations. Eq. 12 is used widely in the literature for opals and inverse opals. Using dynamic diffraction theory, the peak positions change by

$$\lambda_D = \lambda_B \left(1 + \frac{\psi}{2}\right) \quad (11)$$

where ψ is a parameter that can be estimated by

$$\psi = 3\phi \frac{r^2-1}{r^2+2} \quad (12)$$

Here, r is the ratio of refractive indices of the walls and the voids (i.e., $r = n_{\text{walls}}/n_{\text{voids}}$).

It is necessary to remember that, for fcc structures only odds or even indices from planes can reflect light due to the structure factor.^[25]

The structure factor describes the contribution of the entire cell to the diffraction intensity. Each element has its position and, when incident radiation interacts with it, the diffracted wave can interfere destructively or constructively, and certain intensities peaks can be absent.

The structure factor F defines the amplitude of the wave scattered by all the elements of a unit cell divided by the amplitude of the wave scattered by an element.

Consider the position of n_{th} element in the unit cell. The vector \vec{r}_n defines the position in terms of unit vector \vec{a} , \vec{b} , and \vec{c} along x , y , z axes as:

$$\vec{r}_n = x_1\vec{a} + y_1\vec{b} + z_1\vec{c} \quad (13)$$

The path difference between an element at the origin of the unit cell and the n_{th} element is $(\vec{r} \cdot \vec{P})$. And the resultant phase is:

$$\phi = k\vec{r}_n \cdot \vec{P} \quad (14)$$

Where $k = 2\pi/\lambda$ and \vec{P} is the scattering vector, which is the difference between the incident and scattered waves direction. \vec{P} is defined as:

$$\vec{P} = \lambda(h\vec{a}^* + k\vec{b}^* + l\vec{c}^*) \quad (15)$$

The vectors \vec{a}^* , \vec{b}^* , and \vec{c}^* are the basis in the reciprocal space. They are parallel to the basis \vec{a} , \vec{b} , and \vec{c} in the real space.

The structure factor F is the sum of the scattered amplitudes of the individual elements f_n and all the phase differences arising from all path differences, that is

$$F = \sum_n f_n \exp(i\phi_n) = \sum_n f_n \exp(ik\vec{r}_n \cdot \vec{P}) \quad (16)$$

$$\vec{r}_n \cdot \vec{P} = \lambda(hx_1 + ky_1 + lz_1) \quad (17)$$

That is

$$F_{hkl} = \sum_n f_n \exp\{2\pi i(hx_1 + ky_1 + lz_1)\} \quad (18)$$

Intensity is proportional to $|F|^2$ that is

$$|F|^2 = [\sum_i f_i \cos\{2\pi(hx_i + ky_i + lz_i)\}]^2 + [\sum_i f_i \sin\{2\pi(hx_i + ky_i + lz_i)\}]^2 \quad (19)$$

For fcc structures, the reflections are absent if h, k, l indices are mixed odd and even.

This feature is important because, in the spectrum of an opal, the peaks corresponding to the above condition can be detected.

A broad analysis can be made through a dispersion diagram. As mentioned before, due to ratio of therefractive index, colloidal photonic crystals do not have a complete PBG. However, it is possible to observe a frequency interval for wave-vectors lying in the ΓL direction for a reduced frequency window $a / \lambda \sim 0.6$. Incoming light with a wave-vector lying in this crystallographic direction finds no states available to couple with. Light with energies in that range, the so-called “pseudo gap”, cannot propagate through the system in this particular direction. The **Fig. 7** shows the dispersion diagram for opal and inverse opal.

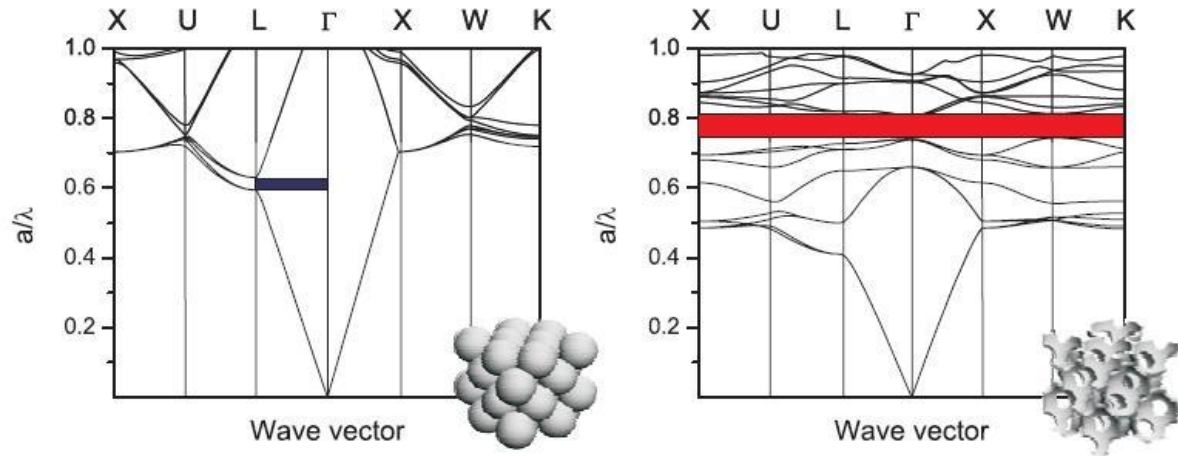


Figure 7. Dispersion diagram for an opal and inverse opal made of SiO_2 . The color areas indicate the incomplete PBG for opal and complete PBG for inverse opal.

1.4 Tunable color in opals and inverse opal photonic crystals

Several mechanisms for generating color in materials are known, including preferential absorption, emission, birefringence, photochromism and other mechanisms. Chromotropism refers to a reversible color transformation in a material due to external chemical or physical influences.^[26] A variety of external stimuli have been demonstrated to produce such color changes. For example, nematic or chiral liquid crystals can change color with temperature or on application of an electric field; other thermochromic materials change color, e.g., when they undergo phase transitions or change molecular configuration as a function of temperature; chemical indicators, such as phenolphthalein, change color with pH, etc. On the basis of this behavior, chromotropic materials have found applications in displays, sensors, information storage, decoration, camouflage and art.

One relatively easy way to obtain materials capable of exhibiting reversible color changes is to use photonic crystals. Among several methods of fabricating such materials have been explored, self-assembly methods that produce three-dimensionally (3D) ordered arrays of monodisperse spheres—so-called colloidal crystals or synthetic opals—as well as inverse replicates of opals or 3D ordered macroporous (3DOM) materials, have been studied intensively.^[27, 28, 29] One of the advantages of colloidal

photonic crystals is their versatility for changing the characteristic reflection peaks in optical spectra (the "stop bands"). The optical reflection peaks are analogous to diffraction peaks in X-ray powder patterns but fall into the submicrometer range instead of the Ångstrom range (**Fig. 8**).

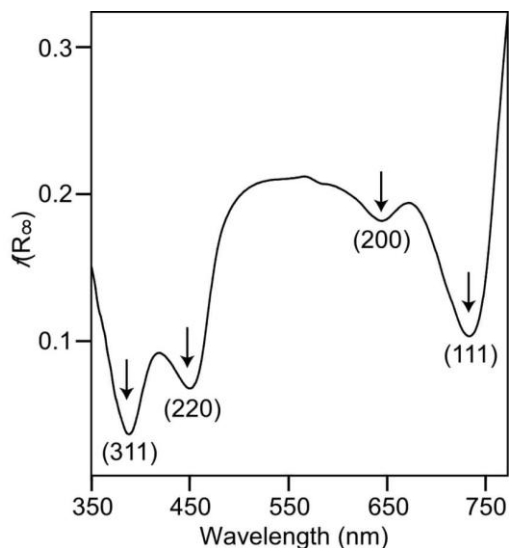


Figure 8. UV-visible reflectance spectrum of a polycrystalline sample of 3DOM mercaptopropyl silica infiltrated with 2-propanol. The stop band minima (marked with arrows) correspond to diffraction from (111), (200), (220) and (311) sets of planes in this photonic crystal with face-centered cubic symmetry (reproduced with permission from Schrodin et al. []. Copyright The American Chemical Society 2002).

In these materials, the stop band positions depend largely on three factors: (1) the refractive index contrast between two periodic media (solid spheres or air spheres and the surrounding phase), (2) the lattice constant (the spacing between spheres) and (3) the filling factor (volume of the spheres compared to the volume of the surrounding phase) (**Fig. 9**). The concept of tunable color in photonic crystals is based on changing the stop band characteristics reversibly through variation of any of these parameters by applying external stimuli.

In this section, we review the diverse routes that have been employed in order to generate reversible color changes based on two structure types: close-packed arrays and non-close-packed arrays. Through appropriate functionalization or structural

modification, each of these structure types can be used to respond to diverse stimuli. Papers that use the term "tunable materials" but merely refer to a change of lattice parameters during the fabrication process or another permanent change in the structure (static tuning), as opposed to responses to external stimuli (dynamic tuning) were not considered here. Reports of tuning of "optical" opals in the IR region rather than the visible range were also not considered.

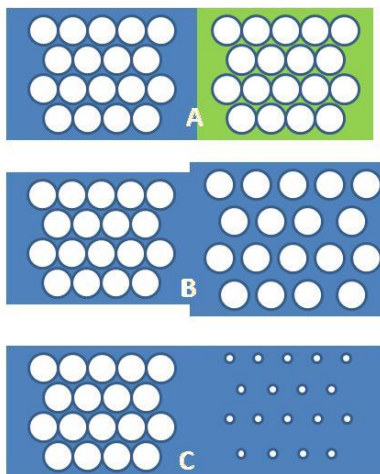


Figure 9. Mechanisms of tuning colors in colloidal crystals: (A) change of refractive index; (B) change of lattice constant; (C) change of filling factor. Spheres are close-packed in case (A) and non-close-packed in the right hand images of cases (B) and (C). See also ref. [18].

Key components in syntheses of both opals and inverse opals are monodisperse spheres, typically composed of silica (SiO_2), polystyrene (PS), poly(methylmethacrylate) (PMMA) or certain block co-polymers. Starting with suspensions of such spheres, close-packed arrays of spheres can be obtained by different methods including centrifugation, sedimentation, vertical deposition, and physical confinement in special cells under sonication.^[30, 31] Inverse opals are usually fabricated by using close-packed sphere arrays as a template and subsequently removing the spheres by pyrolysis or etching methods. These templating methods lend themselves to the fabrication of photonic crystals with a large variety of compositions.

1.4.1 Infiltrated close-packed arrays

In this section we will review several approaches of modifying the average refractive index of periodical structures (opals and inverse opals) by infiltration of the interstitial spaces with secondary phases.

1.4.1.1 Solvents and simple liquids

An early example of photonic crystals with tunable color involved inverse opal photonic crystals, also known as three-dimensionally ordered macroporous (3DOM) materials, composed of ZrO_2 , TiO_2 or SiO_2 .^[32, 33, 34] The samples were in the form of colored powders (**Fig. 10**). Iridescence was observed for larger (millimeter-sized) particles but not for fine powders. Stein and coworkers examined color changes in the materials after infiltration with several organic solvents, changes that could be seen even by the naked eye. They demonstrated that shifts in stop band positions varied directly with the refractive index of the solvent and proposed applications of these materials as solvent sensors or as light-stable pigments.

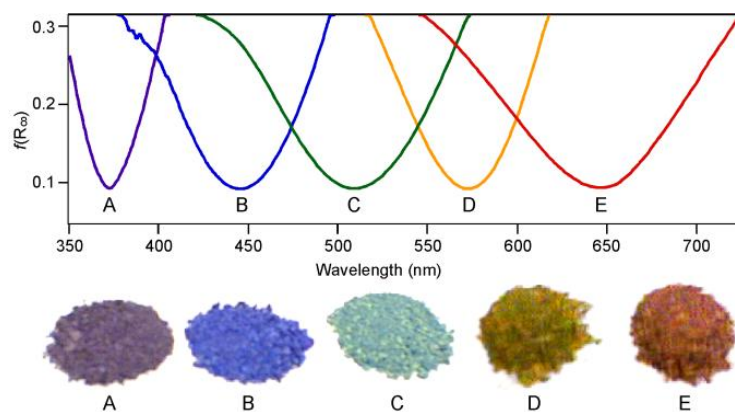


Figure 10. Samples of 3DOM ZrO_2 with different pore sizes (A) 200 nm, (B) 250 nm, (C) 285 nm, (D) sample B infiltrated with methanol, (E) sample C infiltrated with methanol. Corresponding diffuse-reflectance UV-vis spectra are shown above the samples (reproduced with permission from Schroden et al. [34]. Copyright The American Chemical Society 2002).

Ballato and James infiltrated a silica opal with 1-methylnaphthalene, a liquid whose refractive index shows a significant temperature dependence.^[35] The change of refractive index with temperature resulted in changes of light transmission of ~35% over a temperature range of 12 K. Li *et al.* infiltrated silica opals with liquids having melting points near room temperature in order to tune the spectra as a result of changes in refractive index between the liquid and solid phases.^[36] The spectral peaks shifted during solidification by several nanometers, and the shifts were reversible over many cycles of phase changes with a response time of minutes.

Ruhl and coworkers fabricated an interesting multi-component photonic crystal.^[37] They first assembled core/shell structures of silica cores with PMMA shells into an opal by vertical deposition. Titania was then grown in the voids of this opal template by chemical vapor deposition, and the PMMA shells were removed by calcination in air. The product was an inverse opal of titania with silica spheres confined in each pore, so that the voids were partially filled and the pseudo PBG was disturbed. If pores were filled with a liquid whose refractive index closely matched that of silica, such as water, the structure behaved like a standard titania inverse opal filled with a second phase. Hence, simple infiltration switched the photonic band gap. This effect could only be observed if the radius of the silica spheres was within a certain size range relative to the titania macropores.

Liu *et al.* prepared “ternary inverse opals” from PS core/silica shell spheres.^[38] After colloidal assembly and sintering, the hollow silica spheres formed an opal with interstitial spaces available for liquid infiltration. However, the dense shells prevented liquids from penetrating the cores, maintaining a relatively high refractive index contrast in this periodic structure even after infiltration of a liquid phase to tune the stop band positions. In their report, “ternary” referred to the three phases involved in forming the pseudo PBG: air (inside the spheres), the silica shells and the liquids occupying the interstitial space between spheres.

1.4.1.2 Dyes

Spiroyrans and azo-chromophores incorporated in the voids of opal photonic crystals can be used to control refractive indices and optical signals. This property results from their ability to be switched reversibly between *trans* and *cis* isomers by irradiating the material with polarized light of an appropriate wavelength. Gu and coworkers melt-infiltrated the photochromic dyes 1,3-dihydro-1,3,3-trimethylspiro-[2*H*-indol-2,3'-[3*H*]-naphth[2,1-b][1,4]oxazine] or *cis*-1,2-dicyano-1,2-bis(2,4,5-trimethyl-3-thienyl)ethane into silica opal films prepared by vertical deposition on glass substrates.^[39] Photoinduced switching between geometric isomers of the dye resulted in a red shift of the stop band with UV light and a blue shift with light at a wavelength of 600 nm. Although the reflection peak shifted by only 15 nm, the shifts were well controllable with response times of less than a minute.

Hong *et al.* introduced an azo-benzene functionalized polymer [poly(disperse orange 3)] into silica opals and also prepared inverse opals from this polymer.^[40] They showed the ability to shift the stop band to the blue when the azo-polymer was excited by an Ar⁺ laser at 488 nm. Azobenzene groups in the polymer were oriented by the linearly polarized irradiation, and this alignment reduced the effective refractive index of the polymer. Tuning ranges of 40 nm and 20 nm were observed in infiltrated opals and inverse opals, respectively, under the same conditions of laser power and exposure time.

1.4.1.3 Ferroelectrics

In the context of this section, ferroelectrics are materials whose optical transmittance decreases at the Curie temperature because of a phase transition. For instance, between 130–140 °C, BaTiO₃ is converted from the ferroelectric form (cubic cell) to the paraelectric form (tetragonal cell) with an accompanying change in refractive index. Zhou *et al.* took advantage of this property in designing a composite photonic crystal with a thermally tunable PBG. They converted Ba-Ti alkoxide precursors in the interstitial spaces of a silica opal to crystalline BaTiO₃ (refractive index $n \approx 2.5$ at room

temperature) and observed a 20 nm red shift in stop band position at the Curie point (120 °C).^[41]

Kim *et al.* synthesized composite structures of BaTiO₃, PbTiO₃ or SrTiO₃ in the voids of silica opals, using Ba-Ti-ethylhexano-isopropoxide, Pb-Ti-isopropoxide and Sr-Ti-isopropoxide as precursors, which were converted to the oxides after pyrolysis.^[42] The red-shift in the stop band positions depended on the identity of the metal (A) in the ferroelectric perovskite (ATiO₃), being largest for PbTiO₃ (refraction index $n = 2.85$), intermediate for BaTiO₃ ($n = 2.45$) and negligible for SrTiO₃ ($n = 2.176$) as the contrast between refractive indices of both components in the opal composite decreased ($n = 1.46$ for silica).

Li *et al.* prepared a ferroelectric inverse opal composed of ABO₃ material, where $A = (\text{Pb}_{1-x}\text{La}_x)$ and $B = (\text{Zr}_{1-y}\text{Ti}_y)$.^[43] This ceramic material is both transparent and ferroelectric with strong electro-optic effects, and it possesses a high refractive index (2.4–2.6) for visible wavelengths. This material was placed in a cell with indium-tin-oxide (ITO) glass, gold and carbon as electrodes to apply an electric field. A stop band shift of few nanometers was noticed as the applied voltage was raised from 0 to 700 V.

1.4.1.4 Liquid crystals

Liquid crystals (LC) have also been infiltrated into opals and inverse opals. A great advantage of the resulting composites is the ability to control the photonic band gap by either an electric field or by temperature when the molecular orientation of the LC is changed. In their original studies, Ozaki's group infiltrated silica opals with nematic or smectic LC in a cell with ITO windows as transparent electrodes.^[44] They found a change in the photonic stop band position of few nanometers when the temperature was changed. They also studied electric field effects using an alternating voltage (1 kHz) with the nematic liquid crystal 4-pentyl-4'-cyanobiphenyl (5CB) in a silica opal^[45] and in a photopolymer inverse opal.^[46] Above 150 V, a shift and an increase in the intensity of the reflectance peak was detected, but the change was not reversible above this voltage probably due to an anchoring effect of LC molecules in the opal; this "memory" effect disappeared when the material was heated. Importantly, the response

time was shortened compared to conventional systems by encapsulating the LC in the opal voids.

A series of related studies was carried out by Sato and coworkers employing silica opals and inverse opals infiltrated with nematic LC 5CB and placed between two ITO glass slides. They also observed relatively small spectral changes when different potentials were applied.^[47] When the azo dye 4-butyl-4'-methoxyazobenzene was added to the infiltrated LC, irradiation of the colloidal film with UV light induced a *trans-cis* photoisomerization in the azo dye and a molecular re-orientation of the LC from a nematic to an isotropic phase.^[48] This change resulted in an increase in reflectance over a period of several seconds; when the light was switched to white light, the reflectance decreased. The reflectance spectra of silica inverse opals infiltrated with nematic LCs changed dramatically during thermally induced or photoinduced isothermal phase transitions of the LCs.^[49] The response time for the nematic-to-isotropic transition as a function of irradiation intensity was shorter at high intensity than at low intensity.^[50] By combining electric field effects with photo irradiation, it was possible to form images that could be stored for several hours, making such a system promising for use in information storage devices or displays. Sato et al. also studied the effects of linearly and circularly polarized light on SiO₂ inverse opals infiltrated with an azofunctionalized polymer.^[51] They demonstrated that the molecular orientation of azochromophores in polymeric LC could be controlled by polarized light; a shift of 15 nm was possible by switching between the states.

Gu and coworkers prepared a stretched PMMA inverse opal infiltrated with LC 5CB and 4-butyl-4'-methoxyazobenzene.^[52] The LC molecules tended to be orientated in the cavities along the stretched axis, and a clear birefringence effect was noted. Under visible light, a reflection peak was present for polarized light in the direction parallel to the stretching axis but not for light perpendicular to the stretching axis. Under UV irradiation, a blue shift of the reflection peak was observed for polarized light in the direction parallel to the stretching axis, and in this case the reflection peak was also shifted for the perpendicular direction. As UV irradiation altered the isomerization of the azo dye, it reorganized LC molecules from a nematic to an isotropic phase. This

material was proposed to be useful for polarizing devices in displays or beam splitters. An example is a device, which combines LC 5CB, the azo dye 4-butyl-4-methoxyazobenzene, a PS-based opal film and a special mirror.^[53] The color of this device could be tuned over a range of several nanometers. The change occurred under UV irradiation, and the initial state could be regained by application of white light or heat. The size of spheres in the opal determined the original color of the device, the mixture of LC and azo dye acted as the agent for adjusting the color, and the mirror enhanced the reflection.

1.4.1.5 Miscellaneous other systems

Polypyrroles are conductive polymers that can be “doped” by redox processes. Cho *et al.* synthesized opals from silica cores surrounded by polypyrrole shells. This array was sensitive to doping with fuming sulfuric acid, resulting in a reflectance peak shift of 15 nm.^[54] Xu *et al.* prepared polypyrrole inverse opals by infiltrating polypyrrole into a template consisting of spheres with PS cores and PMMA–polyacrylic acid shells by electrodeposition; the template was then removed by extraction with tetrahydrofuran (THF).^[55] The optical properties of the resulting system could be modified reversibly by electrochemical redox reactions in an aqueous LiClO₄ solution inside a cell with ITO windows. The response time was several minutes for a complete reaction.

Cassagneau and Caruso applied the concept of opal infiltration to prepare an optical affinity biosensor for egg-white avidin.^[56] They identified two important requirements for biosensing applications involving affinity reactions: (1) an efficient chemically functionalized matrix to promote further biospecific interactions and (2) a pore size adequate for absorption; inverse opals can satisfy both requirements. The copolymer poly(thiophene-*co*-3-thiophenemethanol) was electrochemically synthesized within the interstices of a PS opal and the template was removed using THF. By controlling the applied voltage during the electropolymerization process, the size of the connecting windows between pores could be adjusted. Biotin was then covalently anchored to the copolymer surface for bioselective recognition of avidin. As the avidin adsorbed to the host surface, it diminished the pore diameter, causing a shift of the optical stop band peak position up to 30 nm.

1.4.2 Superparamagnetic nanoparticle arrays

Colors obtained with superparamagnetic colloidal arrays are tunable without the need for changes in a secondary infiltrated phase. Solvents surrounding such composites can influence the interactions among particles and contribute to refractive index effects that control the material's color, but they do not provide the major external stimulus for dynamic color changes. Instead, a balance of forces among particles dictates the particle assembly, and an external magnetic field permits color tuning in quite a spectacular way. Similarly, in the case of magnetic inverse opals, the alignment of particles relative to the viewing direction is controllable by external magnetic fields and governs the apparent colors.

In early studies, Gates and Xia synthesized magnetite inverse opals.^[57] PS spheres were assembled in a specially designed fluidic cell filled with a ferrofluid containing magnetite nanoparticles (<15 nm diameter). After solvent removal and elimination of the template, a porous magnetic structure (inverse opal) was obtained. Small slabs of this material could be rotated by an external magnetic field when they were placed in an aqueous medium. As the orientation of the slabs changed relative to the detector, different colors were observed consistent with the Bragg diffraction equation.

Asher's group prepared monodisperse superparamagnetic polystyrene-iron oxide composite particles, which formed crystalline colloidal arrays in aqueous solution, aided by the magnetic interactions between particles.^[58, 59, 60] When a magnet was placed near the cell containing the solution, it generated a magnetic field gradient, and the lattice spacing in the periodical particle array was modified, becoming smallest in the regions of highest magnetic field gradient. Several solvents were tested in order to investigate the effects of the dielectric constant on the behavior of the colloidal arrays. For superparamagnetic spheres, colloidal crystallization took place even in aqueous solutions with high ionic strength and in polar organic solvents, conditions that are not favorable for crystallization of nonmagnetic colloidal arrays. The movement of the superparamagnetic colloidal array could be limited by embedding the array in a

hydrogel. When a magnetic field was applied, a shift in the reflection peak position was observed. The hydrogel-embedded system reached equilibrium after one hour.

Similar observations were made by Yin's group for silica-based opal composites whose colors are highly responsive to magnetic fields as external stimuli.^[61, 62, 63] These researchers investigated variations of superparamagnetic composites of the type $\text{Fe}_3\text{O}_4@\text{SiO}_2$, in which a balance between electrostatic repulsive forces and magnetic attractive forces produced ordered arrays of core/shell structures. Diffraction of light from these periodically ordered structures produced the colors; changing the strength of the magnetic field or the thickness of silica shells with the same core size tuned the colors. Assemblies of colloidal nanocrystals were prepared in aqueous solutions,^[64] various polar organic solvents^[65] and also in nonpolar solvents.^[66] The last system is important because many practical applications require non-aqueous solvents, but tuning of the color of colloidal arrays is often difficult in non-aqueous solvents. Color tuning relies on the establishment of strong, long-range repulsive forces, but such long-range forces diminish in non-aqueous solvents. This hurdle was overcome by adding a charge control agent, (bis(2-ethylhexyl)sulfosuccinate), to the non-polar solvent, which produced micelles and enhanced the surface charges of modified core/shell particles. The colors of these systems could be varied in a range of 150 nm by modulating the strength of the external magnetic field.

Superparamagnetic particles have found a practical application in photonic paper.^[67] Magnetically induced self-assembly of $\text{Fe}_3\text{O}_4@\text{SiO}_2$ colloids, followed by UV processing, was used to fix the structure inside a poly(ethylene glycol)diacrylate matrix. A water/ethanol solution of a chloride salt (LiCl , CaCl_2 , MgCl_2) was used as an ink, which swelled the polymer matrix, increasing the interparticle spacing and thereby red shifting the spectrum. Because of their hygroscopic nature, the chloride salts retained moisture in the exposed area. The ink marks could easily be erased by rinsing the paper in distilled water, which dissolved the residual salt, decreased the lattice spacing and produced a blue shift to reestablish the original color. The photonic paper was reusable for several cycles of writing and erasing.

1.4.3 Non-close-packed arrays: Hydrogels

A hydrogel is a flexible network of randomly cross-linked polymers that swells with uptake of water. It has a mechanical response similar to rubber. Generally, sensor structures based on a hydrogel are composites of spheres (usually PMMA, PS or silica) in a polymeric web, where the polymer matrix is modified with covalently attached functional groups capable of reacting with specific chemical moieties. The interactions among molecules create forces that induce swelling or shrinking of the structure; this changes the spacing between spheres and alters the color of the hydrogel. A widely studied hydrogel for this purpose is the thermosensitive polymer poly(*N*-isopropylacrylamide) (PNIPAM), which changes from hydrophilic to hydrophobic behavior at 32 °C. It undergoes a reversible phase transition from a swollen hydrated state to a shrunken dehydrated state, losing 90% of its mass.

1.4.3.1 Temperature

Asher's group pioneered the field of hydrogel-based photonic crystals. In an early report, they described an opal structure of monodisperse particles of PNIPAM, as well as colloidal crystal arrays of PS spheres within a PNIPAM hydrogel.^[68] An opaline PNIPAM film functioned as an optical filter whose extinction coefficient was controlled by temperature as the scattering cross section of the spheres changed. In case of the hydrogel-embedded PS sphere array, both the optical diffraction wavelength and the diffraction intensity changed as functions of temperature. The same group demonstrated optical responses to Pb, Ba and K ions for a composite synthesized by copolymerizing the ion-selective crown ether 4-acryloylaminobenzo-18-crown-6 with nonionic polymerizable monomers within a colloidal PS sphere array.^[69] The tethered crown ether groups localize charge within the hydrogel, which swells in response to bound cations and associated mobile counterions.

Hu *et al.* self-assembled hydrogel nanoparticles of PNIPAM co-polymerized with two different crosslinkers (acrylic acid and 2-hydroxyethylacrylate) and covalently linked together the spheres in the resulting opals.^[70] A color change from green to cloudy white was observed when the hydrogel opal was warmed to 50 °C in an aqueous solution, a

temperature at which phase separation occurred. This change was reversed after only a few seconds of cooling the gel back to 21 °C. A color change also occurred if an electric field was applied while the hydrogel was immersed in deionized water. In this case, electrolysis of water and the resulting ion gradient affected the gel volume. Applications as temperature sensors or as decorative elastic displays were proposed for this system.

Lyon and coworkers studied opals composed of PNIPAM and acrylic acid nanoparticles assembled via centrifugation.^[71] This system displayed Bragg diffraction below the phase transition temperature of PNIPAM; above this temperature, thermally induced disorder of the sphere array shifted the optical diffraction. When the solution was cooled back to room temperature, the crystal reordered itself. In a similar system using *N, N'*-methylene bis(acrylamide) to crosslink the particles, the initial color could be locked in, stabilizing the thermoresponsive behavior over multiple cycles.^[72]

Watanabe's group has investigated a range of different opaline hydrogels that respond to changes in temperature and in certain cases to specific ions. They demonstrated that interconnected sphere arrays exhibited reversible changes in the position of reflection peaks with temperature, whereas spheres embedded in a hydrogel matrix merely changed peak intensity as the temperature was varied.^[73] A PNIPAM inverse opal hydrogel sensitive to both potassium ions and temperature was templated from a silica sphere array using 4-vinylbenzo-18-crown-6 as a potassium-responsive comonomer and *N,N*-methylenebisacrylamide as a cross-linker.^[74] While the porous hydrogel obtained after template extraction responded to changes in temperature, at constant temperature the material also changed color with varying potassium ion concentration. At increasing cation concentration the hydrogel swelled due to a positive internal osmotic pressure created by counterions, as already described earlier for opaline hydrogels modified with crown ether groups. However, a faster response time was noted for the inverse opal hydrogels. It was possible to fine-tune the color in these systems by changing the cross-linker concentration while keeping the size of the templating spheres constant.^[75, 76]

1.4.3.2 Stress

The natural softness of hydrogels makes these materials highly responsive to stresses, which, in turn, produce color changes in hydrogel-based photonic crystals. This "mechanochromic" response results from alterations of the lattice spacing during deformation. Iwayama *et al.* investigated stress behavior in arrays of silica spheres embedded in a disk-shaped poly(acrylamide) hydrogel matrix.^[77] Upon compression, the stop band shifted linearly throughout nearly the entire visible range.

Foulger's group investigated the mechanochromic response of hydrogel-based photonic crystals containing PS particles coated with the photoluminescent dye rhodamine-B as a molecular light source.^[78] They demonstrated coupling between the emission and the stop band. It was possible to vary the stop band position by at least 75 nm, although the intensity was reduced due to disorder in the crystal. The photoluminescence spectrum was blue-shifted by the stress stimulus. The same group tested the Maxwell stress effect with an opal hydrogel.^[79] This effect occurs when a dielectric material is placed in an electric field, and polarization in the molecules charges the surface near the electrodes. If the dielectric material is thin and soft, the Coulombic interactions can induce a stress in the material. For the hydrogel examined, the strain changed the distance between planes of PS particles, and a shift in the wavelength peak was observed. This "electro-mechanochromic" effect was studied in a special cell without and with silver nanoparticles incorporated in the polymer web; the metal affected permittivity in the dielectric and enhanced the strain induced by the electric field. The effect was reversible and could be cycled at frequencies over 100 Hz.

1.4.3.3 pH

Hydrogels capable of sensing ionic species generally can detect changes in pH. Asher *et al.* partially hydrolyzed polyacrylamide hydrogels containing PS crystalline colloidal arrays.^[80] When these hydrogel-based photonic crystal were placed in deionized water, a red shift in the reflection peak occurred as the pH increased; this behavior was due to hydrolysis of amide groups to form carboxyl groups. The ionization of these groups immobilized counter ions inside the gel, resulting in an osmotic

pressure, which swelled the gel against its restoring elastic constant. The maximum hydrogel volume occurred near pH 8.5. The pH and ionic strength dependence of diffraction from these materials could be predicted using an extended Flory's classical ionic polymer swelling model. By using poly(vinyl alcohol) (PVA) as the hydrogel matrix, a pH sensor was obtained that could be reversibly dehydrated and rehydrated while retaining the original diffraction and swelling properties and therefore did not need additives or stabilizers.^[81] A large red shift covering a wavelength range of 350 nm was observed as the pH was raised from 2.6 to 9.1.

Lee and Braun developed a pH-sensitive, inverse opal hydrogel using a mixture of 2-hydroxyethyl methacrylate and acrylic acid.^[82] The response range was related to the concentration of acrylic acid. This material showed hysteresis for increasing and decreasing pH, but the effect disappeared after 20 min. More recently, Wang and Han studied how synthesis conditions affect the kinetic response of inverse opal hydrogels capable of detecting changes in pH, solvents, ionic strength and 1,4 phenylenediamine dihydrochloride (PDA).^[83] Their results agreed with those of Lee and Braun, showing hysteresis and increased sensitivity together with shorter response times as the PDA concentration was increased. The faster response rate is an important factor for sensor applications.

Ueno et al. prepared an electro- and thermochromic copolymer electrolyte hydrogel using methacrylic acid as a pH sensitive monomer, PNIPAM as a thermoresponsive monomer and *N,N'*-methylene bis(acrylamide) as a cross-linker.^[84] In addition to shifting its color in response to changes in temperature, this material revealed interesting behavior when it was placed in water between two electrodes at constant temperature: Before a potential was applied, a reflection peak occurred at 800 nm (transparent and colorless). With an applied potential, electrolysis of water caused a localized decrease in pH near the anode and a pH gradient in the gel. This led to distortion of the colloidal crystal in the gel and a concomitant decrease in the intensity of the reflection at 800 nm. As the volume collapse penetrated the material more uniformly, a new peak appeared at 580 nm (green) within a few minutes. This two-state

color switching could also be observed at different temperatures, and structural colors could be recovered by reversing the applied voltage.

1.4.3.4 Glucose and creatinine

A key for preparing hydrogels with well-defined chemical responses is to surround the colloidal array of spheres with a network that contains molecular recognition elements. Asher's group studied molecular recognition systems that can detect glucose by interactions with boronic acid groups covalently linked to the hydrogel matrix.^[85] These were converted to boronate groups upon binding to glucose or other sugars, which increased the degree of ionization of the hydrogel and thus the hydrogel volume to produce a red-shift. The response of the glucose sensor varied with both pH and sugar concentration in low ionic strength aqueous solutions. A similar concept was applied to inverse opal glucose sensors by Lee *et al.*, who modified a 2-hydroxy-ethyl methacrylate inverse opal with 3-carylamidophenylboronic acid.^[86]

For glucose sensors used in diabetes testing, it should be noted that if a person's blood glucose level on an empty stomach is more than 11 mM, the person is diagnosed as diabetic, and between 7.8 mM and 11mM the person is a borderline diabetic. With this information, Nakayama *et al.* optimized an inverse opal hydrogel for diabetes testing.^[87] They prepared the porous hydrogel with 3-acrylamidophenylboronic acid as the glucose recognition element. The concentration ratio of monomer, cross-linker and solvent was adjusted to obtain a green hydrogel for glucose levels under 7.8 mM, yellow when the concentration was between 7.8 mM and 11 mM, and red for concentrations above 11 mM. This "traffic light" indicates directly the levels of glucose.

Asher's group also modified a hydrogel in order to detect creatinine by a coupled reaction with creatinine deiminase enzyme and 2-nitrophenol groups.^[88] Creatinine clearance is an indicator of renal dysfunction. In this application, creatinine was hydrolyzed by the enzyme, which released hydroxide ions, leading to deprotonation of 2-nitrophenol. The phenolate product was more soluble in the hydrogel, causing it to swell. The net result was a red shift as a function of the creatinine concentration. The

enzyme and 2-nitrophenol are both necessary for the successful operation of this hydrogel.

1.4.3.5 Light

As already noted earlier, photonic crystals can benefit from organic molecules that change their geometry upon exposure to UV or visible light. Kamenjicki *et al.* fabricated PS opals with covalently attached azobenzene groups, which could be photoisomerized to the *cis* form by UV irradiation and returned to the initial *trans* state by white light irradiation.^[89] The *cis* form mixes more readily with the hydrogel, causing it to swell and the reflection peak to red shift by up to 60 nm, depending on the azobenzene concentration. The ability to switch coloration upon exposure to light also permits spatial selectivity, as was illustrated by the synthesis of porous hydrogels with incorporated 4-acryloylaminoazobenzene units.^[90] In another study, Asher and coworkers prepared a hydrogel with spirobenzopyran molecules linked to the hydrogel network.^[91] This molecule can be converted photochemically between the spiropyran (closed) form and the merocyanine (open) form by irradiating the spiropyran with intense UV light or the merocyanine with visible light. The open form relaxes in the dark over periods of days. The radiation-induced switching between the isomeric forms results in red or blue shifts of the stop bands. These are due to changes in charge localization in the attached spirobenzopyran in solvating media, such as dimethylsulfoxide, causing swelling and changes in the lattice constant. Applications for switching or optical memories have been suggested for these systems.

1.4.3.6 Solvents

As we have seen in the earlier examples, hydrogels typically require an aqueous environment for controlled swelling or shrinking. Barry and Wiltzius took advantage of this property as they prepared an acrylamide-based inverse opal humidity sensor.^[92] Humidity variations were achieved by flowing moist nitrogen over the material. When the relative humidity was varied from 20% to 80%, spectral analysis revealed a red shift of approximately 40 nm. For samples exposed to humidity from lower to higher levels, equilibrium was reached in ca. 20 seconds, but the response was slower when the

samples were dried. The structures absorbed water more rapidly than they released the water. Furthermore, the sensitivity of these systems depended on the infiltration time, i.e., the length of time for which an acrylamide hydrogel solution was left in the colloidal crystal prior to cross-linking.

Although water is the main solvent used to support the structure of hydrogels, it is not an exclusive solvent. Takeoka and Watanabe prepared two types of solvent-sensitive hydrogel systems: the first type involved a multicolored gel membrane with non-closest-packed silica nanoparticles in an acrylamide hydrogel cross-linked with *N,N'*-methylene bis(acrylamide); the membrane was readily affected by solvent uptake as an external stimulus, undergoing swelling with water and shrinking with acetone.^[93] The color of the samples could therefore be easily varied by adjusting the acetone/water ratio. The second system involved sphere-templated inverse opals with different PNIPAM/*N,N'*-methylene bis(acrylamide) concentrations.^[94] The swelling ratio of the gels could be expressed as a function of the length of subchains forming the polymer network. The color of the hydrogel photonic crystal was adjustable by changing the cross-linker concentration in the pre-gel solution. Details about this behavior were explained with a theoretical model based on thermodynamic parameters (enthalpy, entropy, volume).^[95] Acrylamide-based hydrogels containing PS sphere arrays have also been shown to respond to ethanol/water mixtures.^[96] These materials showed reduced transmittance and a blue shift covering a wide part of the visible spectrum as the concentration of ethanol was increased. Greater biocompatibility may be achieved by employing a poly(hydroxyethyl methacrylate) hydrogel in a photonic crystal ethanol sensor.^[97]

Wang *et al.* synthesized an inverse opal hydrogel that responded to mixtures of ethanol/water, pH, L-lysine and like most of these soft photonic crystals, to mechanical pressure.^[98] A PS opal template was infiltrated with polyacrylamide (PAM) and polyacrylamide/polyacrylic acid (PAM/PAA). The fraction of polyacrylic acid determined the extent of the blue shift of the reflection peak relative to the inverse opal containing only PAM, making it possible to choose an initial color for the material. PAM is highly hydrophilic and tends to absorb water, but in a mixture of water and ethanol the extent

of absorption is diminished and the reflection peak can be shifted over a range of about 150 nm within the optical region, depending on the ethanol/water ratio. The solvent concentration-dependent shift is different in the PAM/PAA system, due to cross-linking of PAM and PAA through hydrogen bonds. Similar results were found for interactions with urea and L-lysine. The response to pH was nonlinear in this system. At $\text{pH} > 7$ some amide groups in the PAM hydrogel were hydrolyzed to carboxylic groups, swelling the structure due to electrostatic repulsion among carboxylic ions. At $\text{pH} < 7$ the formation of ammonium ions by the protonation of an amide group in an acidic solution led to repulsion among these ionic sites. When acrylic acid was introduced into PAM, the hydrolysis was inhibited.

By exchanging water with other solvents, such as photopolymerizable precursors, it is possible to stabilize multicolor patterns in photonic crystal hydrogels. This was demonstrated by Foulger's group for a system containing PS spheres encapsulated in methacrylate-functionalized polyethylene glycol hydrogel.^[99] Water was removed and replaced with 2-methoxyethyl acrylate as a swelling agent and small amounts of ethylene glycol dimethacrylate and photoinitiator. Subsequent photopolymerization resulted in a water-free robust hydrogel. When a positive photomask was employed during photopolymerization, it was possible to generate colored patterns and even multicolored patterns after a sequence of positive and negative photomask applications. Optical properties could be fine-tuned by selecting appropriate combinations of monomers.

Although these examples have shown that hydrogel-based photonic crystals can respond to a variety of external stimuli, fine tuning of the optical response for sensing is achieved largely by three approaches: (1) changes in the cross-linker density, (2) immobilization of ions in the hydrogel and (3) changes in the free energy of mixing of the hydrogel polymer with the solvent medium. In the first approach, the analyte is bound by two molecular recognition molecules, forming additional cross-links within the gel, causing it to shrink and producing a blue shift in the stop band peak. The immobilization method increases the osmotic pressure and swells the hydrogel, resulting in a red shift. In the third method, a balance between the free energy of mixing

of the hydrogel polymer with the surrounding medium and the elastic restoring force of the hydrogel cross-linkers determines the volume of the hydrogel and the appearance of the photonic crystal.

1.4.4. Non-close-packed arrays: Metallopolymers and Elastomers

Ozin, Manners and coworkers have investigated a range of optically responsive systems based on polyferrocenylsilane, a redox-active metallopolymer with variable degrees of oxidation due to the presence of ferrocene groups. In the first study reported using this material, they used non-connected silica spheres in a matrix of (ethylmethyl)sila-[1]-ferrocenophane cross-linked with sila(cyclobutyl)-[1]-ferrocenophane and sandwiched between two ITO glass slides.^[100] Different solvents were infiltrated into this system. Colors were tuned via two different mechanisms: swelling and changes in the refractive index. In dynamical studies the sample exhibited a relatively fast response, reaching the equilibrium swelling state within 0.2 to 0.4 s. The width of the photonic band gap could be modulated by choosing an appropriate pair of solvents. Taking advantage of the redox activity of polyferrocenylsilane, it was possible to create electrochromic and electromechanochromic composites (so-called "P-Ink").^[101] When an oxidative potential was applied to the composite, electrons were drawn out from the iron sites in the polyferrocenylsilane backbone while anions from the electrolyte were driven into the polymer to neutralize the positive charge buildup. The influx of both ions and solvent in the polymer caused it to swell and push apart the layers of embedded spheres, shifting the optical diffraction peak and the color of the material. A display was constructed, in which the initial colors could be controlled by the fabrication process and later tuned by electric fields. Recently, a better, more efficient system was reported and patented, which could cover a spectral range of 300 nm, almost all of the visible range.^{[102][103]}

Another type of flexible material that has been used with colloidal crystal arrays involves elastomers. The main advantage of elastomers over hydrogels is that they do not require an aqueous environment for handling. Ford's group investigated systems of silica spheres coated with 3-(trimethoxysilyl) propyl methacrylate in either poly(methyl acrylate)^[104, 105] or poly(methyl methacrylate) matrices.^[106] In these crystalline colloidal

arrays the silica particles did not touch each other but were separated by the polymeric matrix. The arrays could be stretched up to 30% uniaxially, resulting in tunable colors. The films were heated to 150 °C and cooled again to room temperature without loss of colloidal crystalline order.

Foulger *et al.* prepared an extended 3D array of monodisperse, crosslinked PS particles within a poly(ethylene glycol) methacrylate matrix.^[107, 108] After drying, the film was swollen in 2-methoxyethyl acrylate. The incorporation of a small quantity of 2,2-diethoxyacetophenone in the re-swollen system followed by photoinitiation with UV light resulted in a completely water-free composite. The color of this system could be tuned when a stress was applied; a shift of almost 120 nm was obtained without any permanent change. The stop bands of this material were studied under static and dynamic conditions, using stresses at different frequencies.^[109] In a related study, Sumioka *et al.* synthesized inverse opals using a mixture of methyl acrylate with PMMA and applied uniaxial stresses in hot water.^[110] The peak wavelength of the stop band changed linearly as a function of the stretching ratio.

Fudouzi and Xia used PS spheres to form an opal structure whose void spaces were infiltrated with poly(dimethylsiloxane).^[111] Exposure to 2-propanol caused swelling of the matrix structure and changed the lattice constant and the color of the elastomer. When the solvent was completely evaporated, the elastomer changed back to its original color. In this way it was possible to switch between two wavelengths. The color could be changed reversibly without any deterioration in quality over 10 cycles. An application of this type of material as a “photonic paper” was proposed.^[112, 113]

Ozin's team synthesized a porous elastomeric film, which could be compressed in one direction with minimal expansion in the other directions.^[114] This resulted in an anisotropic distortion of the photonic crystal film and induced a blue-shift in the stop gap position over a wide range. The material was tested in a biometric recognition device capable of forming images of fingerprints. By incorporating PbS quantum dots in the porous elastomer, photoluminescence of the film could be tuned by deforming the film.

Wohlleben *et al.* explored methods of optimizing the mechanical robustness and elasticity of self-assembled core-shell polymer spheres for photonic devices.^[115] The core shell particles were prepared by two-step or multi-step emulsion polymerization either with hard cores or with flexible cores and film-forming soft shells. Softer cores provided more flexible films but compromised the refractive index contrast slightly. The key of this work was lamination of the colloidal crystal layer over a transparent carrier foil (an acrylic emulsion polymer) in order to enhance the mechanical robustness. A black carrier was chosen to enhance the brilliance of the opalescent top layer. The supported samples could be stretched up to 100% and returned to 50% longitudinal elongation within ca. 2 minutes; the associated color changes covered the complete visible range. Without a carrier, the spheres formed necks, leading to local reductions in film thickness during elongation.

A technique particularly suitable for scale-up of elastomeric opal film production was described by Viel *et al.*^{[116][117]} Using extrusion and melt-flow techniques, complex elastomeric core-interlayer-shell beads were self-assembled into continuous opaline films with a macroscopically ordered fcc lattice. For example, beads consisted of a PS core with a thin interlayer of PMMA and a soft, deformable, outer shell of polyethylacrylate. After extrusion, the colloidal mass was placed between the plates of a press, producing a radial melt flow and organizing the spheres into periodic arrays over large areas. The films were stabilized by photo-cross-linking. When the resulting deformable sheets were placed on a hard, curved mold, they displayed a range of different colors due to differential deformation. Such deformations were reversible up to a critical applied stress. Interestingly, the color intensity was significantly enhanced when carbon nanoparticles were infiltrated in the polymer mixtures.^[118]

1.4.4. Conclusions of tunable color

The examples highlighted above have demonstrated the efficiency and versatility of opals and inverse opal photonic crystals in displaying structural colors, not only as static colors, but also as dynamically variable colors. In all of these systems the production of color relies on a structure whose refractive index varies periodically—in the systems selected here, with three dimensional periodicity generated by arrays of

spheres or voids that are either interconnected or non-close packed and embedded in a matrix.

In most of the close-packed systems, the lattice spacing is relatively fixed, so that tunable color derives largely from changes in refractive index brought about by partial or complete infiltration with another phase (solvents, ferroelectrics, fluorescence compounds, dyes, conductive polymers and liquids crystals). Even if they remain permanently embedded in the pore structures, secondary phases such as liquid crystals provide opportunities for dynamic responses as a function of temperature, pH, applied electric fields, light and chemical species if these stimuli promote changes in the refractive index. The concern that infiltrated phases reduce the refractive index contrast and therefore the structural color intensity has been addressed by designing tertiary phases based on core-shell structures that maintain regions of high refractive index contrast. Some of the most promising applications of these close-packed systems may involve pigments and decorative materials that respond to their environment and profit from the stability of the inorganic components present in these materials.

More flexible photonic crystal structures based on non-close-packed sphere/void arrays in hydrogels or polymeric matrices permit large variations in lattice spacing. Hence, for a given material, color variations can often span a wider range of the visible spectrum, and mechanochromic color formation becomes feasible. Normal hydrogel systems are generally limited to aqueous systems, but with their soft nature and the variety of possible responses (temperature, pH, stress, solvents, moisture, UV and visible radiation and certain analytes, such as glucose or creatinine), they become particularly interesting as sensors for biological systems. Such applications have become feasible with recent developments of biocompatible hydrogel photonic crystals. The versatility of this structure is due to the large selection of possible functional groups that can be attached to the polymeric web and influence the swelling/shrinking of the hydrogel matrix with the associated spectral shifts. In some systems, the extent of the change is very small and may not be appreciated by the naked eye, but it is enough to be considered a tunable material for optical sensor applications.

In terms of mechanical stability and scale-up, elastomeric photonic crystals show perhaps the greatest promise. They build on well-developed fabrication methods for latex-based films while incorporating the benefits of responsive structural colors that are tuned by deformation or local swelling.

The developments over the last decade or so have brought opaline and inverse opal-based tunable photonic crystals to the stage where commercialization has become feasible and the materials are starting to enter the market. Most of the proposed applications for tunable color materials relate to sensors, colorful displays, photonic papers, decorative coatings and responsive packaging. Among these, the requirements for sensors and displays are the most stringent and include a large spectral range, relatively fast response times, mechanical and cycling stability, low voltage/current requirements, and practical, scalable manufacturing process. Progress has been strong in addressing all of these requirements, but opportunities for further improvement exist through both optimization of existing materials and design of novel, complex structures.

Several other interesting systems with periodical structures different from opals and inverse opals have been described that can also produce color but are beyond the scope of this review. These include, for example, one-dimensional columnar charge transfer assemblies in mesoporous silica films,^[119] block copolymer photonic gels,^[120, 121] Bragg stacks,^[122,123] “planar” (2D) photonic crystals,^[124] photonic band gap fiber textiles,^[125] mechanically tunable photonic crystals.^[126] Such structures have generated great interest not only because of their colorful appearance, but also because of other unique optical properties associated with negative refractive elements,^[127] spontaneous emission cavities,^[128] super prisms,^[129] etc. Further advances are anticipated by mimicking biological systems that display structural colors. These do not always require perfect periodicity and can involve complex gradients in periodicity.^[117]

Colors have been important throughout human history. They provide critical functions in both recognition and communication, linking interactions between the animate and inanimate worlds. The artist's palette of color generation mechanisms is relatively large,^[1] but tunable photonic crystals certainly provide unique advantages that complement those of other chromotropic materials.

2. EXPERIMENTAL

2. Experimental

This section is about the experimental set up for preparation samples of colloidal arrays, photonic pigments, photonic paint and the measurements in order to know their optical properties.

Among the different methods for fabricating 3D photonic crystals, colloidal assembly is the easiest. One of the great advantages of synthetic opal is the accessibility for any chemistry laboratory. Photonic crystals by colloidal techniques require two steps: 1) the synthesis of spheres and 2) the mechanism of assembling or crystallization.

Colloidal particles (silica, alumina, titania, polystyrene, polymethylmethacrylate, among others) can be prepared by sol-gel or polymeric methods. For example monodisperse silica colloids are prepared by the well known method developed by Stöber *et al.* ^[130]: tetraethyl orthosilicate (TEOS) is hydrolyzed in ethanol at high pH and produces uniform silica spheres with diameters ranging from 50 nm to 2 μm by adjusting the concentrations of reactants. Uniform latex spheres like PS, PMMA and PMA are mainly synthesized by emulsion polymerization, polymer spheres ranging from 20 nm to 1 μm can be synthesized by controlled concentrations of polymer initiator, temperature, and reaction conditions.

In this work we have worked with polymeric colloidal particles, synthesized by polymerization of methyl methacrylate monomers (**Fig. 11**). Double bonding between carbons is broken for linking with other monomers.

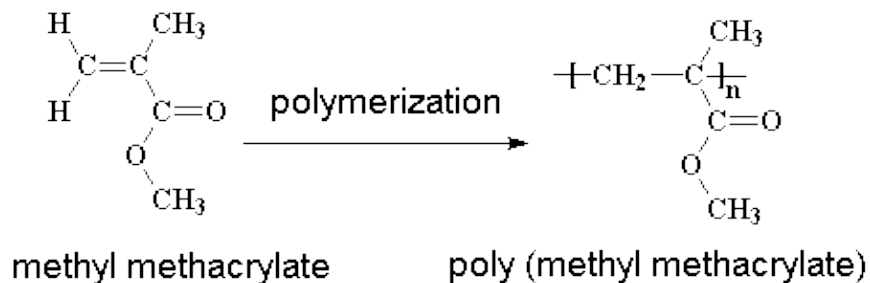


Figure 11. Polymerization of methyl methacrylate molecule.

2.1 Synthesis of spheres

Methyl methacrylate (99%, Aldrich) and 2,2 azobis (2-methylpropioamidine) dihydrochloride (97%, Aldrich) were used for the preparation of PMMA spheres. Carbon black (acetylene black, Chevron Phillips Chemical Company) and commercial Chinese ink (Higgins® Fontain Pen India non-waterproof black ink Sanford Corp.) were employed as carbon sources. Deionized and charcoal-treated water (18.2 M Ω .cm specific resistance) was used for all sample solutions.

The procedure used was a modification of the method reported by Schroden *et al.*^[34] Monodispersed poly(methyl methacrylate) spheres were synthesized by emulsion polymerization of a rapidly stirred aqueous suspension activated with an azo initiator water soluble.

80 ml of D. I. water and 15 ml of methyl methacrylate are placed in a three necks round bottom 250 mL flask and stirred with a 20 x 10 mm oval-shaped magnetic stir bar, a mercury thermometer under a slow flow of nitrogen. The nitrogen enters through a long needle and exits through a short needle passing through a stopper in the top of a condenser and then to a bubbler to monitor flow (2.3 ml/s). Corning stirrer-hotplate spins the stir bar at constant speed and keeps the temperature at 70 °C. The system is placed inside a crystallizing dish containing water, which helps minimize temperature fluctuations (**Fig. 12**).



Figure 12. Set-up for synthesis of PMMA spheres.

After a constant temperature of 70°C is achieved, 0.1 g of the initiator is added to the solution, maintaining a 70°C temperature and rapidly stirring. The initiator 2,2-azobis(2-methylpropionamidine) dihydrochloride is added through the neck where the thermometer was put, since adding it to a joint that was exposed twice to methyl methacrylate vapor results in a joint permanently fused with poly(methyl methacrylate). A milky white suspension is observed as the polymerization proceeds.

The size of the spheres produced depends on temperature, stir rate, and concentration. For the samples reported, only the stir rate was varied in a range of 100 RPM to 300 RPM; although the other variables were explored too, with similar results. After 60 minutes at constant temperature, the suspension is transferred to centrifuge tubes. There should not be a noticeable odor if the polymerization was successful.

2.2 Assembly of opal structures

There are several methods of sphere assembly: sedimentation, centrifugation, vertical deposition, electrophoresis, packing cells, spin annealing. ^[131]

The method we used was the centrifugation process. Samples generated with this method have a high amount of disorder (dislocations, stacking faults, mosaic spread), which usually spoil the optical performances of the system, but it is very easy and relatively quick. Those who seek fewer defects usually prefer using other methods, mainly vertical deposition.

In the centrifugation process, colloidal suspension in tubes is placed inside a centrifuge machine over a 12 hrs period at a constant speed, in a range typically between 1000 to 2000 RPM. After this time, the tubes are decanted and the sample is dried under laboratory conditions. It takes approximately two days to dry completely; the result is a monolith which looks white with little colorful sparks in some areas; the small uniform diameter particles should appear iridescent if they are close-packed and their size is similar to the wavelength of visible light. The monolith can be broken into fine particles and a white powder is produced. This whiteness is due to scattering among different regions.

2.3 Mixtures of carbon with opaline powders: photonic pigments

The experiments with carbon were inspired by the experimental observation that spreading opaline powder over any dark surface gives coloration. After that we eliminated the large dark background surfaces, and tried to achieve similar effects just by addition of carbon to the opaline powders.

Two different sources of carbon were used: carbon black powder and Chinese ink (or Indian ink). Carbon black can be fabricated in two ways, by incomplete combustion and by thermal decomposition of organic matter. It essentially consists of elemental carbon in the form of nearly spherical particles of colloidal size, coalesced into particle aggregates.^[132] India ink is a dispersion of carbon black in water, stabilized with alkaline solutions.^[133]

Two methods were using for producing mixtures of PMMA with carbon nanoparticles. In the first, different amounts of carbon black powder (concentrations between 2-8 wt.% were suitable to obtain the desirable color effects) were mixed with a fixed amount of PMMA opals in a porcelain mortar, crushed and sieved through a 200-mesh sieve to produce particles in a dispersion size of a range from 20 to 75 μm .

The second way was using monolithic pieces of PMMA opals (known mass, each piece several mm on each side), which were infiltrated over a period of a few hours, depending on wt. % (from 2 to 4 hrs.) with different amounts of commercial Chinese ink; the original concentration (wt. 0.00189 gr/ml) was obtained after water evaporation. Afterwards these samples were crushed and sieved through a 200-mesh sieve. The powders produced will be referred to as “photonic pigments”

2.4 Preparation of photonic paint

Since colored powders without iridescence to the naked eye were produced, they were considered as pigments, and then paint could be prepared with this new pigments. A basic paint is a combination of pigment for coloring, with a polymer to form the layer and a solvent as liquid vehicle. The problem with our colored powder is its porosity; any permanently infiltrated liquid into the structure destroy the color effect.

After testing different polymers, a commercial solution of polyvinyl acetate, PVA (used commonly as carpenter glue) by *Henkel Mexicana S.A de C.V* was a good solution; D.I. water was used as the solvent. Testing different combinations of proportions, we found the optimum to be: 0.16 to 0.25 g/ml (half of mass of photonic pigment and half of PVA) from translucent layers to opaque layers.

The paint was applied in two different ways for different objectives. The first applications were on different surfaces with a little brush just to observe the same color appearance in powders and paint without any control of thickness. The paint was applied on a piece of bond paper, a piece of glass and a piece of wood; the last one was chosen for applying the paint and testing iridescence.

A controlled layer thickness (100 μm) was applied to white photographic paper for measuring spectra in order to obtain Scattering and Absorption coefficients and for testing transmission over glass slides.

In order to know additional parameter for defining optical properties of paints layers (thickness 150 μm) with different concentrations were deposited on glass slides. Intensity measurements were taken by the test fiber optic probe in mode intensity and a diode laser (wavelength 656 nm) was used as source of light. The intensity was measured for five conditions: initial beam light, through a single glass slide, through PVA solution layer, and through three paint samples (0.16 g/ml) for pigments of three different carbon concentrations. **Figure 13** shows the homemade apparatus for the controlled deposition over a glass surface or photographic paper.

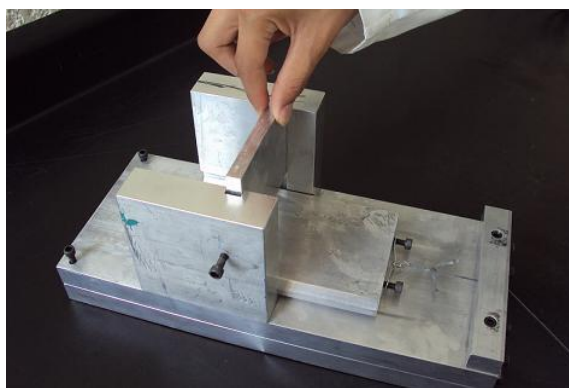


Figure 13. Homemade mechanical apparatus for depositing uniform layers of paint

2.5 Instruments

The samples were analyzed using UV-Vis spectrophotometer with a fiber optic probe model *Jaz* and the software *Spectra Suite* both of them by *Ocean Optics*. Spectra were obtained for randomly oriented bulk powder samples at a normal incidence to the powder surface. SEM images were obtained using JEOL 6500 and JEOL JSM-6390LV scanning electronic microscopes. Particle diameters were estimated from the SEM images.

Visual images were taken with a Nikon Coolpix[®] S220 digital camera (10 Mpixels) with flash light inside a dark box in order to avoid undesired reflections from surroundings.

The software used for analyzing the spectra was used to obtain the chromatic coordinates. The graphics of absorption and scattering coefficients versus wavelength were calculated with Kubelka - Munk's theory using reflectance data.

The paints applied over a piece of wood were analyzed in order to detect iridescence, with a common set up taking spectra at different angles. In **Fig. 14** L is white collimated light source, S is the sample of paint applied to a wood surface, f is the test fiber optic probe, sm is the spectrophotometer, the notation θ_{α} , means illumination angle (θ) and measure angle (α).

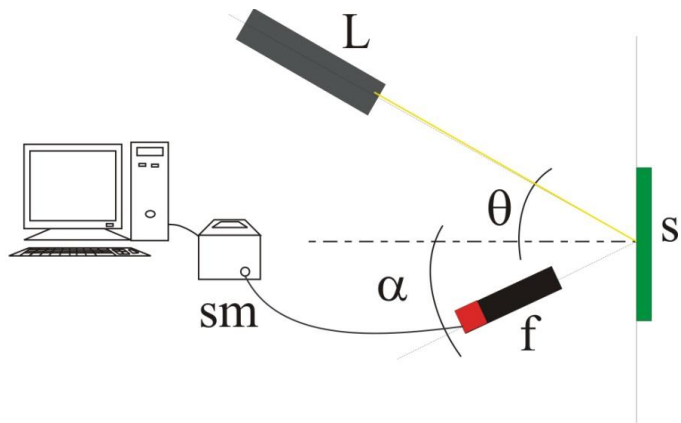


Figure 14. Set up used for analyzing the iridescence of photonic paint.

3. RESULTS AND DISCUSSION

3. Results and discussion

3.1 Colloidal Photonic Pigments with Low-Angle-Dependence

The powder obtained without carbon looked white, but powdered mixtures prepared with PMMA opals and carbon black appeared uniformly opaque and matte without any iridescent color observable by the naked eye. **Figure 15** shows visual images of typical powders and SEM images of the powder and a particle. Typical colloidal crystals grains have dimensions between a few micrometers and tens of micrometers.

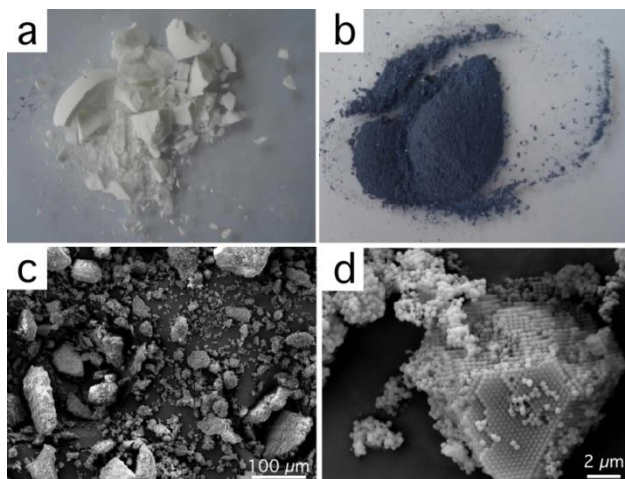


Figure 15. A colored powder results from mixing PMMA colloidal crystal arrays with carbon nanoparticles, here producing a sample of blue color. a) Photograph of PMMA colloidal crystal array powder without carbon. b) Photograph of powdered PMMA colloidal crystal array with carbon. c) SEM image of the blue powder which has a wide distribution of particle sizes limited by the 200 mesh sieve. d) SEM image of a particle where it is possible to observe the opal structure.

Samples for different spheres size were synthesized. **Figure 16** shows three different colored powders and their corresponding UV-vis spectra, in which the color depends on the different sizes of spheres composing the colloidal crystals.

Several interesting features of the spectra can be noted. Each spectrum consists of a series of reflection peaks in the UV-vis-IR range, associated with the periodic

structure of the randomly oriented colloidal crystal particles. Sample colors arise from the sum of these peaks in the visible range. Although, the expected order of colors would be green, blue and then violet with decreasing sphere diameters, the observed order is blue (diameter size 340 ± 10 nm), purple (diameter size 310 ± 10 nm), and green (diameter size 240 ± 10 nm) due to superposition of multiple reflection peaks.

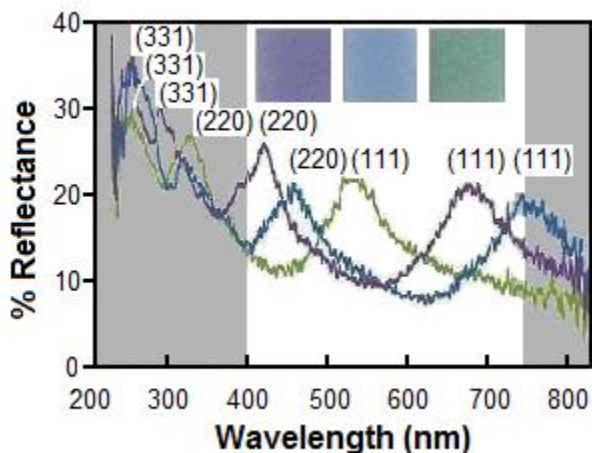


Figure 16. Diffuse reflectance spectra for different colored powders composed of mixtures of PMMA colloidal crystals and 5 wt. % carbon black powders. The gray areas correspond to regions outside of the visible spectral range. The insets show photographs of the purple powder (diameter size of PMMA spheres 310 ± 10 nm), blue powder (diameter of PMMA spheres 340 ± 10 nm) and green powder (diameter size of PMMA spheres 240 ± 10 nm). The periodic peaks in each spectrum result from the fcc structure of the colloidal crystals. The sample purple has a red component.

The colored powders produced were mainly purple, blue and green. It was not possible to obtain pure yellow, orange or red colors, although several changes in synthesis conditions were made. This puzzling result was analyzed.

From Eq. 9 and Eq. 10 it is possible to calculate the reflected peaks in the spectrum corresponding to specific sphere diameter, considering a refractive index for PMMA of 1.4914 at 587.6 nm.^[134] Table 1 shows the peaks of the corresponding planes (111), (220) and (331) for sphere diameter from 200 to 400 nm.

Size diameter	Peak from (111)	Peak from (220)	Peak from (331)	Color appearance
200	444.17	272	176.49	purple
210	466.38	285.6	185.32	blue
220	488.59	299.2	194.14	cyan
230	510.80	312.8	202.97	green
240	533.0	326.4	211.79	green
250	555.21	340	220.62	green
260	577.42	353.6	229.4	yellow
270	599.63	367.2	238.27	orange
280	621.84	380.8	247.09	orange
290	644.05	394.4	255.92	red
300	666.26	408	264.74	reddish purple
310	688.46	421.6	273.57	reddish purple
320	710.67	435.2	282.39	reddish purple
330	732.88	448.8	291.21	reddish purple
340	755.0	462.4	300.04	blue
350	777.30	476	308.86	cyan
360	799.51	489.6	317.69	green
370	821.72	503.2	326.51	green
380	843.93	516.8	335.34	green
390	866.13	530.4	344.1	green
400	888.34	544	352.99	green

Table 1. Color appearance corresponding to size diameter of spheres. The gray cells correspond to regions outside of the visible spectral range. The appearance in visible range of electromagnetic spectrum can be the first peak, the second peak or a combination of peaks.

If the sphere diameter is less than 300 nm, the color appearance, corresponding to the first peak (111) depends proportionally on the diameter of spheres, as they usually have been reported in the literature. But, if the sphere diameter is greater than 300 nm, the color is determined by the second peak corresponding to (220) or a combination of the first and second peaks in the visible range. Seeing Table 1, it is possible to understand our results related to the sample colors: pure yellow, orange and red are less probable than the other colors; these colors require more careful conditions in their synthesis to be achieved.

Increasing the carbon content in the range from 1–8 wt% resulted in more intense coloration. Above 8 wt% or below 1 wt%, the mixtures were too dark or too white, respectively, to see well defined colors. Different chromatic coordinates can be adjusted in this range. **Figure 17** shows photos and their respective spectra of three different carbon contents for a sample labeled as purple (diameter size 320 ± 10 nm).

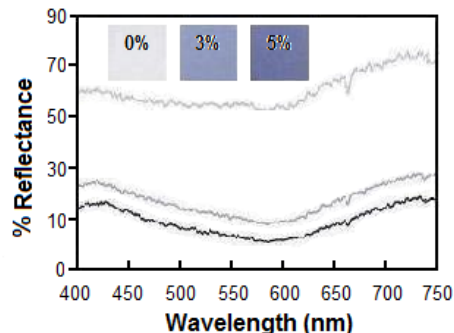


Figure 17. Diffuse reflectance spectra and photographs (insets) for different concentrations of carbon black in mixtures with PMMA opaline powders correspond to a purple sample (diameter size of PMMA spheres 322 ± 10 nm).

Samples with the same mass of solids from India ink appear similar to samples mixed with carbon black in color hue, but they do not appear as dark as the mixtures with carbon black. **Figure 18** shows spectra and photographs for samples mixed with carbon black powders and samples infiltrated with India ink.

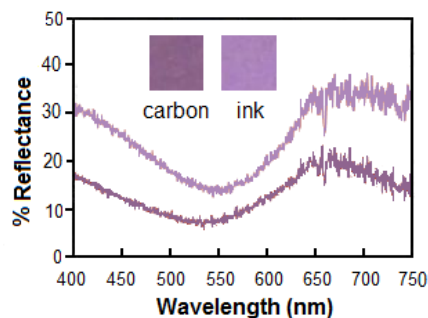


Figure 18. Diffuse reflectance spectra and photographs (insets) for different carbon source: carbon black powders and India ink at the same loading of dry mass; PMMA opaline powders correspond to a reddish purple sample (diameter of PMMA spheres 315 ± 10 nm). The hue color appearance is similar but the sample with carbon black looks darker than the sample with India ink.

The difference in luminance of both powders can be due to the lower amount of carbon in the dried ink for the same mass of carbon black. Ink is composed of coated carbon particles to avoid agglomerates when particles are put in water. The dry mass measured from the ink is carbon with other unknown components; the appearance of dry ink is brilliant in comparison with carbon black, which is opaque. It is possible to obtain the same coloration using carbon black powder and black India ink adjusting amount of dry mass respect to carbon; in the end, the effect is the same: mixtures of carbon and opaline powder result in colored powder.

Carbon black can be fabricated in two ways, by incomplete combustion or by thermal decomposition of organic matter. It essentially consists of elemental carbon in the form of nearly spherical particles of colloidal size, coalesced into particle aggregates. **Figure 19** shows an SEM image of carbon black where it is possible to observe that the size of carbon black nanoparticles is less than 100 nm.

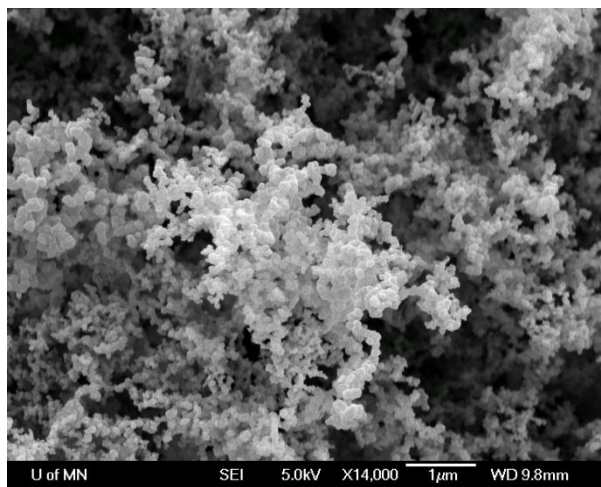


Figure 19. SEM image of agglomerates of carbon nanoparticles whose diameter size is less than 100 nm.

According to the SEM image, carbon nanoparticles do not fill the interstices and do not cover all opal domains; they are merely attached to the surface of colloidal crystal particles in limited regions. **Figure 20** shows a SEM image of a photonic particle.

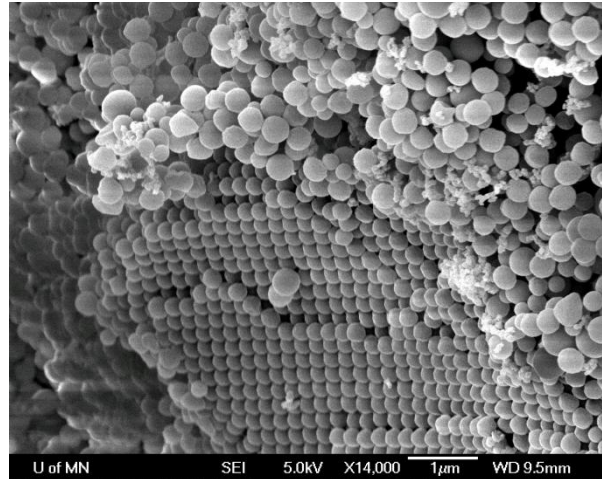


Figure 20. Carbon nanoparticles are attached to the surface of photonic particles in some areas. Due to their size, the carbon particles cannot penetrate into interstices of opal arrays but are present only on defect sites or on the external particle surface.

Do the carbon particles absorb certain wavelengths for coloring? No, carbon powder does not work to produce color effect as a selective absorber. Its spectrum does not show a preferential absorption for any wavelength in the UV-vis range (**Fig. 21**).

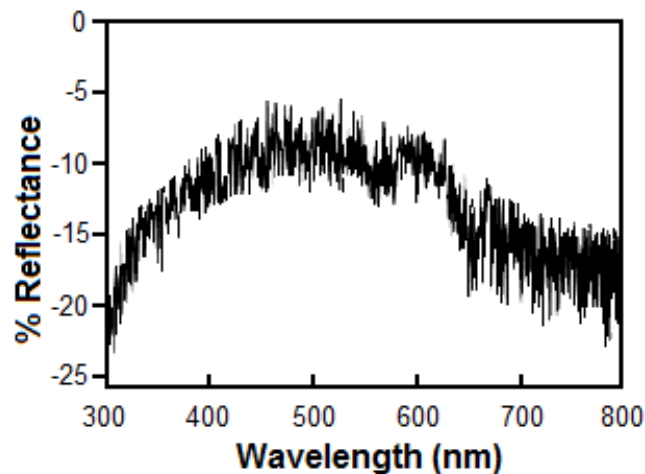


Figure 21. Spectrum of carbon black powder. Carbon does not show preferential absorption in the UV-vis range. Therefore the opal structure is responsible for the color effect.

Spheres made of silica ($n = 1.5302$)^[135] were synthesized, opal arrays were formed, mixtures with both sources of carbon were achieved and color powders were produced, as well, with similar appearance. The main advantages for making photonic pigments with silica spheres is the tolerance of this material to high temperature and its environmental friendliness.

Inverse opal powders made of silica were used for some samples, but in the crushing for making the mixture, the grains were broken, due to the structural weakness. Photonic pigments made with inverse opals made of TiO_2 , ZrO_2 , SiO_2 were proposed by Stein group^[34], they look iridescent and do not need carbon; a little amount of carbon particles enhances coloring, but carbon does not have an important role in their coloration. We are currently looking at the effect of carbon remaining from the template on the color of 3DOM oxides. Samples containing residual carbon are much more intensely colored.

PMMA and silica are transparent in the visible range and carbon black does not have any preferential absorption, therefore just the opal structure is the main factor in producing the color effect. It is very interesting that colored powders made with polymer and carbon can exhibit coloration just through optical phenomena.

These colored powders could be good candidates for new pigments. The main problem with our colored powder is its porosity; any permanently infiltrated liquid within the structure alter the color and can completely eliminate the color if the refractive index of the solvent is closely matched to that of the photonic crystal.

We found that a commercial solution, based on polyvinyl acetate (PVA) mixed with D.I. water was a good solution. After optimization of the composition, from 0.16 to 0.25 % m/v (half of mass of color powder and half solid mass of PVA over a volume of D.I. water) was used to apply, with a brush, a layer on different surfaces. When the mixture of PVA solution, water and photonic pigments is made, a dark liquid is formed, and just when solvent evaporates and dry powder surrounding by solid PVA is deposited over the substrate, the color returns. **Figure 22** shows examples of the application on a piece of paper and on a piece of wood for the color powders shown in

Fig. 16. Photos of paper were taken using the flash light of the camera inside a black box, and the photo of the piece of wood was taken under diffuse natural light of the laboratory.



Figure 22. Paint resulted of a mixture of D.I. water, solution based on polyvinyl acetate and the colored powders. Photograph of paint applied on different surfaces, i.e., paper and wood.

The paints have a matte appearance similar to the powders and look rough. The two features of the appearance are due to several photonic grains randomly held by a polymer layer (**Fig. 23**). The thickness of applied paint is more than $100\ \mu\text{m}$ and the typical mean size of grains is $40\ \mu\text{m}$ (statistics made from SEM image).

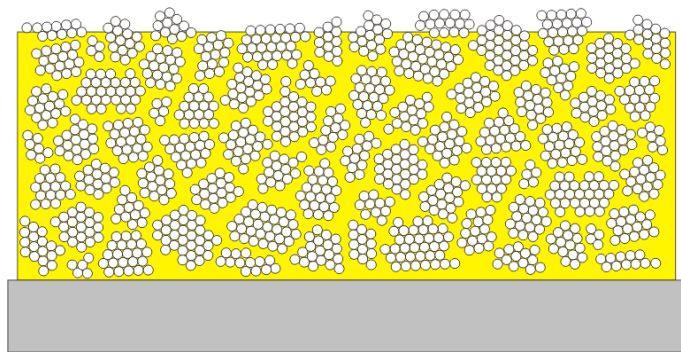


Figure 23. Scheme of deposited paint over a flat surface. The roughness of paint suggests some superficial particles hold by polymer layer. The polymer layer is around particles. The image is not proportional to real dimensions

Other photonic paint has been reported by McGrath *et al.* That paint uses poly (styrene-co-N-isopropylacrylamide) and shows iridescence ^[136]; our paint is composed of more simple elements and its appearance is uniform to the naked eye.

Could the paint have a certain iridescent effect which is not noticed by the naked eye? To answer this question the setup shown in Fig. 14 was used for measuring the spectra at different angles; the notation θ_α , means illumination angle (θ) and measuring angle (α). The green paint applied on the wood surface was used to measure the spectra. We took spectra at different angles of illumination and angles of measurement, and the behavior was similar; **Figure 24** shows just the spectra at 10° of illumination.

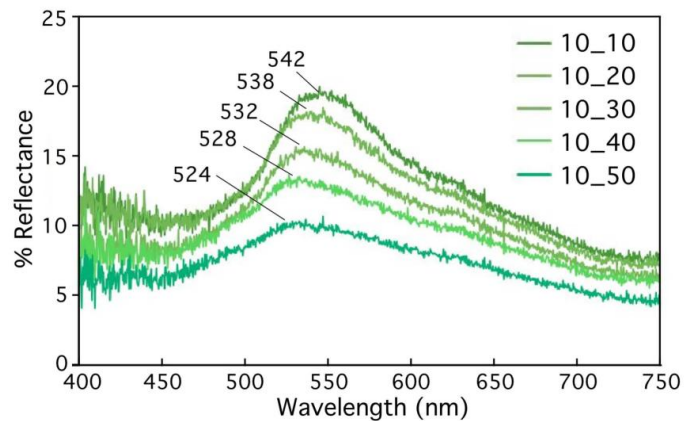


Figure 24. Blue shift of reflectance diffuse spectra of paint applied over wood surface show an iridescent effect, the total shift of 18 nm is not appreciable to the naked eye. The legend indicates the illumination angle (first number, always 10°) and the measurement angles (second number, between 10 and 50°).

The peaks have a blue shift at: 542 nm (10_10), 538 nm (10_20), 532 nm (10_30), 528 nm (10_40), 524 nm (10_50), a total difference of 18 nm over 40°, it is not possible to notice any color change with the naked eye; therefore photonic pigments have a low-angle-dependence. Photonic materials with low-angle-dependence appearance have been reported. Takeoka and coworkers developed a hydrogel membrane with 2–4% wt of polymer, which displayed a constant color over a viewing angle of 40° ^[137]; those angles are greater than we reported.

We analyzed the color behavior of the purple samples shown in Fig. 17, using the common convention of chromatic coordinates. The *Commission Internationale de l'Eclairage* (CIE) accept different color spaces, one of them being $L^*a^*b^*$ (based on nonlinearly compressed CIE XYZ color space), which indicates the colors by three factors: luminance (L^*), red-green axis (+a to -a) and yellow-blue axis (+b to -b). The coordinates (obtained by software) for the purple samples containing different carbon loadings are shown in Fig. 23. Varying fractions of carbon affect all three coordinates, not only luminance. On the basis of these numbers, it is possible to reproduce similar colors of powders with common design software.

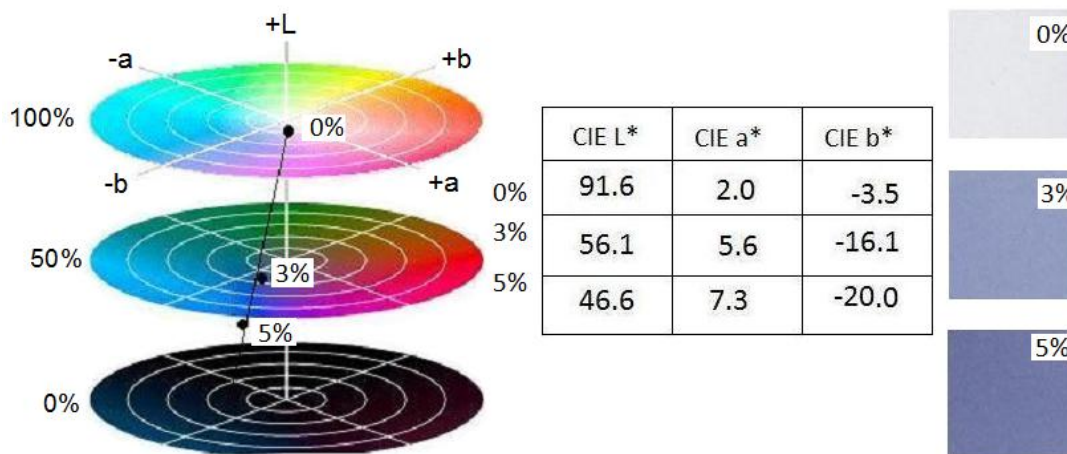


Figure 25. Chromatic coordinates at CIE $L^*a^*b^*$ space of color powders at different carbon wt % corresponding to the samples in Fig. 17.

The phenomenological theory about color refers to all statements about how the radiance of light incident on a layer is affected by absorption and scattering. We used the Kubelka and Munk theory, in order to determine the absorption coefficient (K) and scattering coefficient (S) as a function of wavelength, using spectra information.

If a pigment layer is thick enough (we used 5 mm), the incident light just scatters and one does not see the underlying background layer. It is then possible to apply Equation 20, where R_∞ is the reflectance of an infinitely thick layer; this relationship depends on wavelength. Using Eq. 20 and the spectra shown in Fig. 17, we obtained the K/S curve (**Fig. 26 a**).

$$\frac{K}{S} = \frac{(1-R_\infty)^2}{2R_\infty} \quad (20)$$

The K/S relationship can be useful in certain applications; in our case we need the behavior of each parameter. First the spectrum of (R_0) of a white photographic paper was measured. After, a controlled thick layer ($h = 100 \mu\text{m}$) of paint was applied over the white surface and its spectra (R) was taken; each paint layer measured had a defined carbon content. Finally we used that spectra and the reflectance spectrum of an infinitely thick layer of powder (R_∞) for calculating the constants K and S following Eq. 21 and Eq. 22. [8]

$$a = \frac{1}{2} \left(\frac{1}{R_\infty} + R_\infty \right) \quad b = a - R_\infty \quad (21)$$

$$S = \frac{1}{bh} \operatorname{arccoth} \left(\frac{1-a(R+R_0)+RR_0}{b(R-R_0)} \right) \quad K = S(a - 1) \quad (22)$$

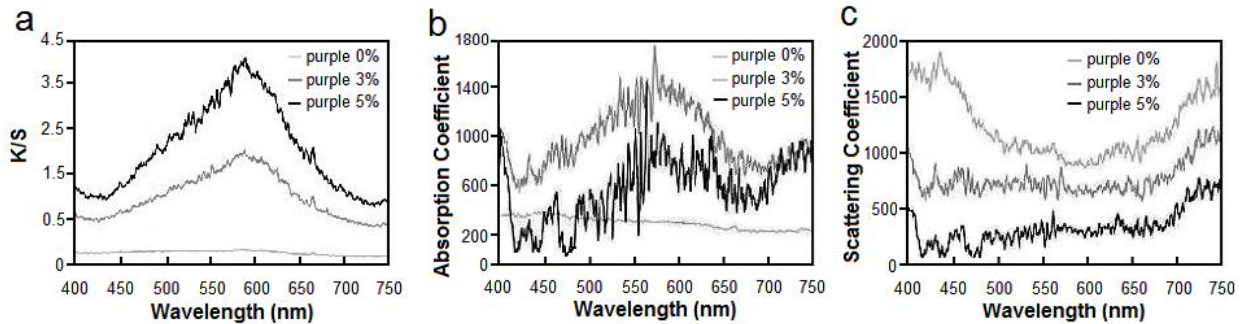


Figure 26. Optical properties of paints made with photonic pigments at different carbon wt %. of Fig 15: a) Ratio of absorption to scattering coefficient (K/S) as a function of wavelength. b) Absorption coefficient as a function of wavelength ($K(\lambda)$). c) Scattering coefficient as function of wavelength ($S(\lambda)$).

When the sample does not contain carbon, scattering predominates, absorption is almost zero, and the curve of the absorption coefficient as a function of wavelength ($K(\lambda)$) is flat. Increasing the carbon content of the samples disturbs this behavior. In case of the scattering coefficient as a function of wavelength ($S(\lambda)$), it is possible to notice a “smoothing” tendency, the curve for purple (0 wt% carbon) follows the form of the spectrum and has the maximum values, and a decreasing is shown with higher

carbon content. The verification that curves are correct is determined by taking the K coefficient over S coefficient for each wavelength and recovering the K/S curve.

Another approximation to get information about scattering and absorption contribution of photonic pigments is by intensity of transmitted light.

In far field range the irradiance is attenuated according to:

$$I = I_0 \exp(-\alpha_{ext} h) \quad (23)$$

Where h is the thickness of sample and α_{ext} is attenuation coefficient; it is proportional to the extinction cross section (C_{ext}):

$$\alpha_{ext} = \mathfrak{N} C_{ext} \quad (24)$$

Where \mathfrak{N} is the number of particles where interacting with incident light. In order to know an idea about how many particles can scatter in a measurement, they were estimated taken a volume of paint of layer of lighted area ($A = 7.85 \times 10^{-7} \text{ m}^2$) and thickness of layer paint ($h = 150 \times 10^{-6} \text{ m}$) the maximum volume is $1.17 \times 10^{-10} \text{ m}^3$. If we consider a volume of a cubic particle of $a = 40 \times 10^{-6} \text{ m}$, and if all particles were uniform and packed together they will be around 1800, we only will take 1500 particles.

The extinction cross section (C_{ext}) is defined as the ratio of power energy through an involving from a particle to incident irradiance; therefore its unit is square meter and physically is composed of scattering cross section (C_{sca}) and absorption cross section (C_{abs}) by:

$$C_{ext} = C_{abs} + C_{sca} \quad (25)$$

If a sample does not have carbon $C_{ext} = C_{sca}$, the absorption cross section (C_{abs}) is produced with Eq. 25 supposing that C_{sca} is the same for all samples. We assume that C_{ext} for PVA and the glass substrate is the same in all measurements. The values of C_{ext} and C_{sca} for paint samples using the pigments in Fig. 17, paint concentration of 0.16 % gr/ml are shown in Table 2.

Sample	C_{sca} [m ²]	C_{abs} [m ²]	C_{ext} [m ²]
Paint with purple 0%	- 2.83	0	- 2.83
Paint with purple 3%	- 2.83	-1.62	- 4.45
Paint with purple 5%	- 2.83	-3.69	- 6.52

Table 2. Values of extinction cross section (C_{ext}), scattering cross section (C_{sca}) and absorption cross section (C_{abs}) from paints using photonic pigments at different carbon wt % of Fig 25.

3.2 Elements for modeling the color effect of colloidal photonic pigments with low-angle-dependence

In this work it has been mentioned that the color came from the opal structure but two questions remain to be clarified: 1) how do carbon nanoparticles work in the photonic pigments? And 2) why do the opals (with defects) exhibit coloration almost without iridescence if the structure itself does not have a complete PBG?

The color effect of photonic pigments with low- angle-dependence involves several optical processes. We can discuss the phenomenon at two levels: light interacting with a single photonic particle (assembly of spheres with absorption) and light interacting among photonic particles.

3.2.1 Optical effects of opals with extinction

Even though each sphere has the same angular distribution, the behavior of an assembly depends on the way the spheres are packed together. The scattering of a single sphere is modeled thorough the use of Mie solution for Maxwell equations. If a second sphere is placed in the vicinity of the first one, the situation becomes more complicated due to interference effects between the scattered waves emerging from both scatters. Let us imagine N spheres close one to another; we have a multiple scattering process. If the spheres are placed in a periodic array, the multiple scattering yields to the incomplete PBG; numerical calculi of PBG by different approaches have been made ^[138]

An incomplete PBG, means that only light with defined wavelength at specific incident angles with respect to structure will be reflected in the structure (**Fig. 27**); mathematically the Laue condition have to be satisfied:

$$\vec{k}' - \vec{k} = \vec{G} \quad (26)$$

Where \vec{k}' is the wave vector associated with reflected light by structure, the wave vector associated to incident light and \vec{G} is the vector in reciprocal space associated to planes (hkl) ; we mentioned in section 1.3 that only planes with odd or even indices can reflect light; obviously \vec{G} is relating with those planes by an easy transformation.

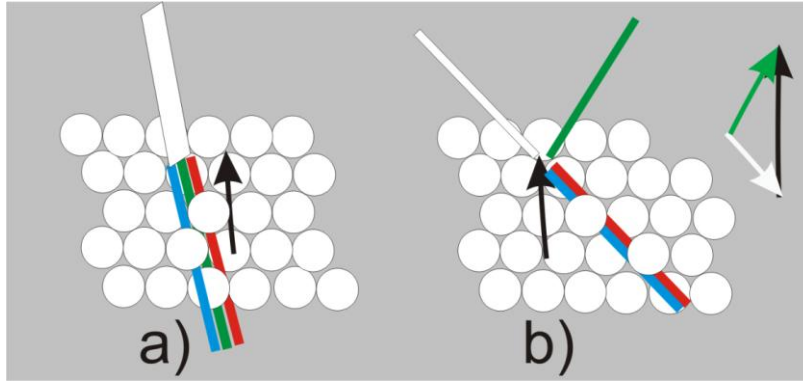


Figure 27. Interaction between a white beam light and a photonic crystal with an incomplete PBG (opal array): a) if Laue condition is no satisfied incident light pass through the structure. b) Light is reflected for specific wavelength only if Laue condition is satisfied. The white arrow is the incident wave vector, green arrow is the reflected wave vector and black arrow is \vec{G} associated to direction of a plane.

All synthetic opals have defects to some degree; the effect of defects on opal arrays has been studied and reported in literature. ^[139, 140, 141] The defects broad the bands in the dispersion diagram and diminishing the transmission exponentially as a function of slab thickness.

The materials used for spheres in opals generally do not have absorption in the visible range; however opals with absorption have been studied. ^[142] Usually absorption is modeled as an imaginary part of the refractive index, the values of absorption have to be in some range, because great number produces an effect metallic opal. The effect of absorption in opals is that the transmission is thickness dependent; Dorado and Depine

conclude that “a perfect photonic crystal with material absorption generates almost the same reflectance and transmittance as disordered photonic crystals without material loss”.^[143]

Both scattering and absorption remove energy from a beam of light passing through the medium: the beam is attenuated; this attenuation is called extinction.^[144]

In the opals we used extinction as an important ingredient; the scattering is due to defects and the absorption of carbon nanoparticles attached to the surface. The total effect of extinction in opals has to do with diminishing the intensity of transmitted light through the structure in forward direction.

The carbon nanoparticles mixed with synthetic opals had not been reported in the way that we applied them. The literature provides evidence that carbon nanoparticles can be used for enhancement of structural color. Pursiainen *et al.* reported that sub-50 nm carbon nanoparticles, which were uniformly incorporated in a highly ordered polymeric (elastomer) colloidal crystal, enhanced its color.^[145] Wang and coworkers found color enhancement in an anodic aluminum oxide film with nanochannels (similar to a diffraction grating) that was coated with an external carbon layer.^[146] The appearance of pearlescent pigments is also enhanced by carbon nanoparticles.^[147]

Although carbon nanoparticles generate extinction, both absorption and Rayleigh scattering, with the model of the color effect they are not considered to be independent scatters, but their absorption property is taken into account as the imaginary part of the effective refractive index of the array.

Let's imagine a perfect opal array (without defects) placed over a dark surface, and a white beam light interacts with. If the Laue condition is satisfied, a reflected light appear and the transmitted light is absorbed by the dark surface. With the opals we make, the carbon nanoparticles are randomly distributed and cover some small areas over the surface of each opaline particle. The transmitted light is not absorbed drastically but it is diminished exponentially in forwards direction (**Fig. 28**)

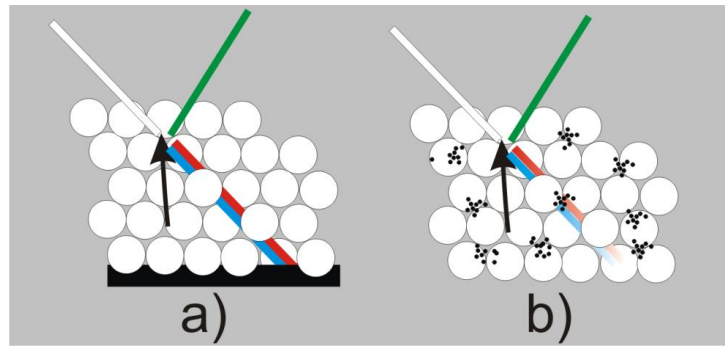


Figure 28. Scheme of absorption effect in opals. a) If a dark surface backs an opaline particle, the transmitted light is absorbed and just reflected light is detected. b) The carbon nanoparticles do not cover the surface of particle but diminishes the light intensity whereas light pass through structure. The arrow means the direction of a plane.

3.2.2 Multiple scattering by photonic particles

If one looks at an opal array deposited carefully over a rigid substrate, iridescence of the sample connected to the Bragg reflection is exhibited, but away from PBG the system does not look transparent, its appearance is white.

The color powder is composed of “photonic particles” (opals with carbon nanoparticles attached to them) of different size (greater than wavelength), shapes and random orientation; it is an ordered –disordered powder.

There are different approaches to model the scattering of a random media composed of many particles. ^[148, 149] Usually the scattering problems are not easy; each one requires certain boundary conditions for solving. To model the scattering of a group of particles, it is necessary to take into account the size, shape and the refractive index. Although each photonic particle is ordered (it has a *fcc* array), the difficulty level increases because each one is composed of hundreds of spheres and its shape is irregular and each one has different size; first problem: the particles in the sample are non homogeneous in shape and size.

The particles that participate in the scattering do not have a constant refractive index. The refractive index inside an opal structure depends on the direction of the photonic crystal and is calculated by group velocity, defined as:

$$n = \frac{v_g}{c} \quad (27)$$

$$\mathbf{v}_g = \nabla_{\mathbf{k}}\omega \quad (28)$$

Where n is the refractive index, v_g is the group velocity, which can be calculated as 3D derivate of frequency with respect to the wave vector.

The complexity increases if both reflected and transmitted light depends on incident wavelength and orientation with respect to opaline particles; the orientation affects the Laue condition as well as polarization. A model of scattering by “traditional methods” is complicated.

Another route to explore the behavior of light inside of an opaline powder is multiple scattering. Multiple scattering occurs when light is scattered several times in succession before it emerges from the medium, each particles exposed to light scattered by other particles. This regime is applied when the average distance between two scattering events (the mean free path ℓ) is much smaller than the sample dimensions.

The multiple scattering of light has a very complicated solution in terms of Maxwell equations when many scatters have to be taken into account. A way to solve this problem is the radiative transfer equation of the dilute medium where phase and light interference are neglected.

The diffuse approximation of light can be viewed as a diffusion process. The most important parameter is the scattering mean free path ℓ_s , which is the average distance between two consecutive scattering events. This parameter sets the limits of the diffusive approximation: $\lambda \ll \ell_s \ll L$ and $k \cdot \ell_s \gg 1$ where L is the sample thickness

and k is the wave vector. After several scattering events, the light propagation is completely randomized.

The whole diffuse transport may be truncated by absorption, which is introduced in the diffusion equation through the inelastic scattering term $\tau_i = v_e/\ell_i$ where the absorption time τ_i is the characteristic time over which light is absorbed in the sample.

When the material which composes the system presents absorption, its effect is increased by a diffusive propagation. The inelastic absorption length ℓ_i is the average depth by which light propagates ballistically in an homogeneous medium before being attenuated by a factor e . The diffusive absorption length ℓ_a is the distance light propagates diffusively before being absorbed. Inside a diffusive and absorbing material is the penetration depth of the diffuse light. Diffuse light propagates a greater distance than in a homogeneous material to reach the same depth. For this reason, ℓ_a is shorter than ℓ_i . However, both are not independent functions but are related to ℓ_t as

$$\ell_a = \sqrt{(\ell_t \cdot \ell_i)/3} \quad (29)$$

The scattering mean free path in opals has been produced. In those works it was found that the total light transmission is directly proportional to the transport mean free path and inversely proportional to the slab thickness. ^[150, 151]

Similar experiments could be achieved for photonic pigments and a value for mean free path could be deduced, however the multiple scattering itself does not solve the problem about why photonic particles generate a color effect.

3.2.3 Combination of optical phenomena

The big difference in this study with respect to others about opals is the role of order. Other opal systems are always deposited carefully over a rigid substrate, where the planes (111) are always oriented parallel with respect to surface. In contrast, photonic pigment powders are composed photonic particles of different sizes, shapes and are oriented randomly.

Although the reflection and transmission light in each particle behaves in the same way (as is shown in Fig. 27) and the size and shape essentially do not affect the reflectance, the randomness in orientation generates many different planes (111), (220), (331) and so on, and can be oriented in some ways that light can always interact with.

In the interaction of photonic particles, transmitted light interacts more with the structure than the reflected light. Both of them are diminished by absorption property of carbon nanoparticles but the forward light diminishes more than the backward light because reflected light does not penetrate inside structure; for this reason the color reflected can “survive” with respect to other wavelengths. The multiple scattering enhances reflected light and produces an effect of diffuse light almost in a Lambertian way (Fig. 29).

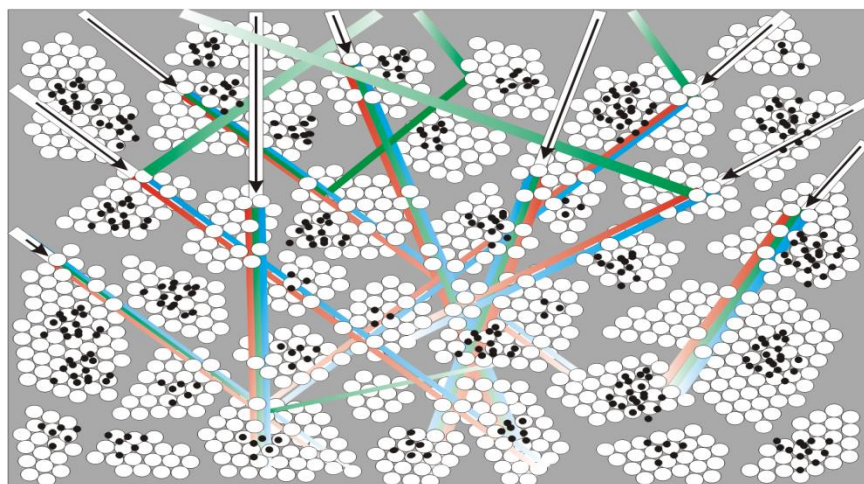


Figure 29. Scheme of interaction of light with photonic particles. The combination of optical phenomena (Fig. 25 and Fig. 26) explains the color effect in opal powders mixed with carbon nanoparticles. The arrows indicate the incident white light direction.

The peaks relate to diffraction planes in the UV-vis-IR spectra from pigments (Fig. 18 and Fig. 16), the scheme of interaction of light with opaline particles (Fig. 27) and the results reported by the Asher group ^[152, 153] suggest a similarity between this phenomenon and diffraction of crystalline powders.

In diffraction of powders, X-rays with defined wavelengths interact with the crystalline planes of each particle oriented randomly, the signal from the sample is measured at different angular positions (scanning in the space) exhibiting peaks with certain amplitudes. In photonic powders, light of different wavelengths interact with planes of each particle oriented randomly, the signal from the sample is measured at the same position (scanning in spectrum), exhibiting peaks with certain amplitude.

With traditional pigments light of certain wavelengths is reflected and others are absorbed; both mechanisms essentially take place at molecular bonding levels (quantum phenomena). In the photonic pigments with low-angle-dependence a similar processes occurs, but in this case the reflection is produced by an incomplete PBG and multiple scattering, whereas absorption (or extinction) is produced by carbon nanoparticles and structural defects (optical phenomena).

4. CONCLUSIONS AND FURTHER WORK

4. Conclusions and Further work

The application discussed in this work uses the well known opal structures reported since 1995 as a practical photonic system. The novelty here is the use of a powder composed of opaline particles with defects and with carbon nanoparticles attached to each which generate an interesting color effect not reported before.

In summary, there are two main results of this study:

1) We have developed a new kind of pigment that could be called “photonic pigments with low-angle-dependence”. Although these new pigments are based on opals (which means iridescence), their appearance to the naked eye is a uniform matte color; this is the main difference with respect to patented photonic pigments which change color to angle view. The photonic pigments with low- angle- dependence imply: saving money in fabrication costs due to a variety of colors with a few chemical compounds; the use of not so common compounds in the pigment industry (PMMA and carbon); the non bleaching by UV radiation and the possibility to have “green photonic pigments” (if they are made with silica spheres); and a potential use in commercial paints.

2) We have discovered a new mechanism of coloration involving a combination of different optical phenomena: incomplete PBG + multiple scattering + extinction. The incomplete PBG generates reflected light from opals just from certain directions and certain wavelengths; multiple scattering contributes with the randomness of orientation of particles and therefore a diffuse distribution of backward light; extinction implies diminishing light intensity more in forward than backward directions with respect to incident light direction.

The photonic pigments with low-angle-dependence are not “universal pigments” for all applications. There are two main weaknesses of this system compared to traditional pigments and paints: 1) it is impossible to make color with subtractive (or additive) mixtures, for example, a blue photonic paint mixed with a red photonic paint does not result in purple photonic paint because the color came from an optical effect;

and 2) if the incident light is low in intensity, the color of the powder is hard to distinguish.

The immediate next work is the numerical simulation of the previously commented phenomena: the optical behavior of one opaline particle depending of size, shape and the scattering by random particles with special way (PBG) to reflect and transmit light.

Further work could be done in the direction of industrial fabrication: the calculation of costs of scalability for a pilot plant; the research for suitable applications and competitive advantages with respect to commercial pigments; the study of limitations for specific industrial applications.

Another way to deeply explore photonic pigments with low-angle-dependence could be as IR filter paint. Nowadays, IR filters are made by dielectric stacks (1D photonic crystal) which are carefully deposited over a prepared glass. An IR paint based on spheres with sizes greater than 500 nm could be studied for filtering; the idea is to apply a layer of photonic IR with brush or pistols instead of a dielectric stack deposition.

Disordered opals, called photonic glass ^[154, 155], could be applied as filler in white paints in order to diminish the amount of titania of paint. It will be necessary to analyze its compatibility with other components of the paints and the advantages of this system respect to other fillers.

Some research groups are researching into order-disorder systems based on opal structures; for instance, random lasers and emission effects, optical properties of photonic glass percolation fractals and light transport on partially ordered configurations. The study we made could be considered to be an order-disorder system, as well.

Photonic crystals have opened a fascinating route to explore materials with new optical properties: photonic optical fibers, resonant cavities, confining spaces for modifying quantum properties, filters, optical cloaking, etc. There is intense scientific activity in this area. Theoretical and experimental works on photonic crystals have built

the foundations for the beginning of an era of new commercial applications based on periodic and semi-periodic structures at wavelength scale.

After almost of 15 years of world research on colloidal photonic crystals, it is amazing how opal has been a structure so versatile: made with different materials, interesting composites, close and non close arrays, inverse structures, ordered and disordered systems, doped with quantum dots, infiltrated with liquid crystals and different solvents, etc. Our work, opaline powders with carbon nanoparticles, is joined to other studies about opals as a little brick in the building called photonic materials.

5. REFERENCES

5. References

- ¹ Nassau K. in *The Physics and Chemistry of color, The fifteen causes of color, 2nd Ed.* John Wiley & Sons Inc. **2001**
- ² Born M. and Wolf E. in *Principles of Optics 7th ed.* Cambridge University Press **1999**
- ³ Pfaff G.; Reynders P. Angle-dependent optical effects deriving from submicron structures of films and pigments *Chem. Rev.* **1999**, 99, 1963
- ⁴ Srinivasarao M. Nano-optics in the biological world: beetles, butterflies, birds, and moths, *Chem. Rev.* **1999**, 99, 1935
- ⁵ Kinoshits S.; Yoshioka S. Structural color in nature: The role of regularity and irregularity in the structure *Chem Phys Chem* **2005**, 6, 1442
- ⁶ Vukusic P.; Sambles J. R. Photonic structures in biology. *Nature* **2003**, 44, 852
- ⁷ Völz H. G. in *Industrial Color Testing. Fundamentals and Techniques.* VCH Germany **1995**
- ⁸ Vukusic P.; Stavenga D. G. Physical methods for investigating structural colours in biological systems *J. R. Soc. Interface* **2009** 6, 133
- ⁹ Kubelka P.; Munk F. Ein beitrag zur optic der farbanstrische Z. *Tech Phys.* **1931** 12, 593
- ¹⁰ Joannopoulos J. D.; Jonhson S. G.; Winn J. N.; Meade R. D. in *Photonic Crystals, Molding the flow of light 2nd Ed.* Cambridge University Press, England **2008**
- ¹¹ Prather D. W.; Shi S.; Sharkawy A.; Murakoswki J.; Schneider G. J. in *Photonic Crystals, Theory, Applications, and Fabrication* John Wiley and Sons New Jersey, USA **2009**
- ¹² Kittel C. in *Introduction to Solid State Physics* 8th ed. Wiley **2005**
- ¹³ Yablonovitch E. Inhibited spontaneous emission in solid state physics and electronics *Phys. Rev. Let.* **1987**, 58, 2059
- ¹⁴ John S. Strong localization photons in certain disordered dielectric superlattices *Phys. Rev. Let.* **1987**, 58, 2486
- ¹⁵ Busch K.; Lölkes S.; Wehrspohn R. B. and Föll H. in *Photonic Crystals: advances in design, fabrication, and characterization* Wiley –VCH **2004**
- ¹⁶ Astratov V. N.; Bogomolov V. N.; Kaplyanskii A. A.; Prokofiev A.V.; Samoilovich L. A.; Samoilovich S.M.; Vlasov Y. A. Optical spectroscopy of opal matrices with CdS embbeded in its pores: quantum confinement and PBG effects, *Il Nuova Cimento D* **1995**, 17, 1349

-
- ¹⁷ Busch K.; John S. Photonic band gap formation in certain self-organizing systems *Phys. Rev E.* **1998**, 58, 3896
- ¹⁸ Rodriguez-Moraz S. I.; Albrecht T.; Anselmann R. "Pigments" CA2408990 2002-11-15
- ¹⁹ Munro C.; Merritt M. D.; Lamers P. H. "Color effect compositions" US2003125416 2003-07-03
- ²⁰ Wulf M.; Taennert K.; Allard D.; Zentel R. "Preparation of specific color effect pigments of photonic crystals" WO 2006116640 2006-11-02
- ²¹ Liu Z-F.; Ding T.; Zhang G.; Song K.; Clays K.; Tung C-H. Ternary inverse opal system for convenient and reversible photonic band gap tuning *Langmuir* **2008**, 24, 10519
- ²² Aguirre C. I., Reguera E., Stein A. Tunable colors in opals and inverse opal photonic crystals. *Adv. Func. Mater.* **2010**, 20, 2565
- ²³ Blanford C. F.; Schroden R. C.; Al-Daous M.; Stein A. Tuning solvent dependent color changes in three dimensionally ordered macroporous (3DOM) materials through compositional and geometric modifications *Adv. Mater.* **2001**, 13, 26
- ²⁴ Vos W. L.; Sprink R.; van Blaaderen A.; Imhof A.; Legendijk A.; Wegdam G. H. Strong effect of photonic band structures on the diffraction of colloidal crystals *Phys. Rev. B* **1996**, 53, 16231
- ²⁵ Tilley Richard J. D. in *Crystals and Crystal Structures*, John Willey and Sons, USA, **2006**
- ²⁶ Y. Fukata (Ed.) in *Inorganic Chromotropism. Basic Concepts and Applications of Colored Materials*, Kodansha Springer, Tokyo **2007**
- ²⁷ Special issue on photonic crystals. *Adv. Mater.* **2001**, 13, 6, 369-450
- ²⁸ J. C. Lytle, A. Stein in *Annual Reviews of Nano Research*, ed. by G. Cao, C. J. Brinker, Vol. 1, World Scientific Publishing Co. 1-79, **2006**
- ²⁹ A. Stein, F. Li, N. R. Denny, *Chem. Mater.* **2008**, 20, 649
- ³⁰ Y. Xia, B. Gates, Y. Yin, Y. Lu, *Adv. Mater.* **2000**, 12, 693
- ³¹ S. Furumi, H. Fudouzi, T. Sawada, *Laser & Photonics Rev.* **2010**, 4, 205
- ³² C. F. Blanford, R. C. Schroden, M. Al-Daous, A. Stein, *Adv. Mater.* **2001**, 13, 26
- ³³ C. F. Blanford, H. Yan, R. C. Schroden, M. Al-Daous, A. Stein, *Adv. Mater.* **2001**, 13, 401
- ³⁴ R. C. Schroden, M. Al-Daous, C. F. Blanford, A. Stein, *Chem. Mater.* **2002**, 14, 3305
- ³⁵ J. Ballato, A. James, *J. Am. Ceram. Soc.* **1999**, 82, 2273
- ³⁶ J. Li, W. Huang, Z. Wang, Y. Han, *Colloids and Surfaces A* **2007**, 293, 130
- ³⁷ T. Ruhl, P. Spahn, C. Hermann, C. Jamois, O. Hess, *Adv. Funct. Mater.* **2006**, 16, 885
- ³⁸ Z.-F. Liu, T. Ding, G. Zhang, K. Song, K. Clays, C.-H. Tung, *Langmuir* **2008**, 24, 10519

-
- ³⁹ Z.-Z. Gu, T. Iyoda, A. Fujishima, O. Sato, *Adv. Mater.* **2001**, *13*, 1295
- ⁴⁰ J.-C. Hong, J.-H. Park, C. Chun C., D.-Y. Kim, *Adv. Funct. Mater.* **2007**, *17*, 2462
- ⁴¹ J. Zhou, C. Q. Sun, K. Pita, Y. L. Lam, Y. Zhou, S. L. Ng, C. H. Kam, L. T. Li, Z. L. Gui, *Appl. Phys. Lett.* **2001**, *78*, 661
- ⁴² B. G. Kim, K. S. Parikh, G. Ussery, A. Zakhidov, R. H. Baughman, E. Yablonobitch, B. S. Dunn, *App. Phys. Lett.* **2002**, *81*, 4440
- ⁴³ B. Li, J. Zhou, L. Li, X. J. Wang, X. H. Liu, J. Zi, *Appl. Phys. Lett.* **2003**, *83*, 4704
- ⁴⁴ K. Yoshino, Y. Shimoda, Y. Kawagishi, K. Nakayama, M. Ozaki, *Appl. Phys. Lett.* **1999**, *75*, 932
- ⁴⁵ Y. Shimoda, M. Ozaki, K. Yoshino, *Appl. Phys. Lett.* **2001**, *79*, 3627
- ⁴⁶ M. Ozaki, Y. Shimoda, M. Kasano, K. Yoshino, *Adv. Mater.* **2002**, *14*, 514
- ⁴⁷ Q.-B. Meng, C.-H. Fu, S. Hayami, Z.-Z. Gu, O. Sato, A. Fujishima, *J. Appl. Phys.* **2001**, *89*, 5794
- ⁴⁸ S. Kubo, Z.-Z. Gu, K. Takahashi, Y. Ohko, O. Sato, A. Fujishima, *J. Am. Chem. Soc.* **2002**, *124*, 10950
- ⁴⁹ S. Kubo, Z.-Z. Gu, K. Takahashi, A. Fujishima, H. Segawa, O. Sato, *J. Am. Chem. Soc.* **2004**, *126*, 8314
- ⁵⁰ S. Kubo, Z.-Z. Gu, K. Takahashi, A. Fujishima, H. Segawa, O. Sato, *Chem. Mater.* **2005**, *17*, 2298
- ⁵¹ M. Moritsugu, S.N. Kim, T. Ogata, T. Nonaka, S. Kurihara, S. Kubo, H. Segawa, O. Sato, *Appl. Phys. Lett.* **2006**, *89*, 153131
- ⁵² Z.-Y. Xie, L.-G. Sun, G.-Z. Han, Z.-Z. Gu, *Adv. Mater.* **2008**, *20*, 3601
- ⁵³ G.-Z. Han, Z.-Y. Xie, D. Zheng, L.-G. Sun, Z.-Z. Gu, *Appl. Phys. Lett.* **2007**, *91*, 141114
- ⁵⁴ G. Cho, M. Jung, H. Yang, B. Lee, J. H. Song, *Materials Letters* **2007**, *61*, 1086
- ⁵⁵ L. Xu, J. Wang, Y. Song, L. Jiang, *Chem Mater.* **2008**, *20*, 3554
- ⁵⁶ T. Cassagneau, F. Caruso, *Adv. Mater.* **2002**, *14*, 1629
- ⁵⁷ B. Gates, Y. Xia, *Adv. Mater.* **2001**, *13*, 1605
- ⁵⁸ X. Xu, G. Friedman, K. D. Humfeld, S. A. Majetich, S. A. Asher, *Adv. Mater.* **2001**, *13*, 1681
- ⁵⁹ X. Xu, S. A. Majetich, S. A. Asher, *J. Am. Chem. Soc.* **2002**, *124*, 13864
- ⁶⁰ X. Xu, G. Friedman, K. D. Humfeld, S. A. Majetich, S. A. Asher, *Chem. Mater.* **2002**, *14*, 1249
- ⁶¹ Y. Lu, Y. Yin, B. T. Mayers, Y. Xia, *Nano Lett.* **2002**, *2*, 183
- ⁶² J. Ge, Y. Hu, Y. Yin, *Angew. Chem. Int. Ed.* **2007**, *46*, 7428
- ⁶³ J. Ge, Y. Hu, T. Zhang, Y. Yin, *J. Am. Chem. Soc.* **2007**, *129*, 8974
- ⁶⁴ J. Ge, Y. Hu, T. Zhang, T. Huynh, Y. Yin, *Langmuir* **2008**, *24*, 3671
- ⁶⁵ J. Ge, Y. Yin, *Adv. Mater.* **2008**, *20*, 3485
- ⁶⁶ J. Ge, L. He, J. Goebel, Y. Yin, *J. Am. Chem. Soc.* **2009**, *131*, 3484

-
- ⁶⁷ J. Ge, J. Goebel, L. He, Z. Lu, Y. Yin, *Adv Mater.* **2009**, *21*, 4259
- ⁶⁸ J. M. Weissman, H. B. Sunkara, A. S. Tse, S. A. Asher, *Science* **1996**, *274*, 959
- ⁶⁹ J. H. Holtz, S. A. Asher, *Nature* **1997**, *389*, 829
- ⁷⁰ Z. Hu, X. Lu, J. Gao, *Adv Mater.* **2001**, *13*, 1708
- ⁷¹ J. D. Debord, L. A. Lyon, *J. Phys. Chem. B* **2000**, *104*, 6327
- ⁷² J. D. Debord, S. Eustis, S. B. Debord, M. T. Lofye, L. A. Lyon, *Adv. Mater.* **2002**, *14*, 658
- ⁷³ M. Kumoda, M. Watanabe, Y. Takeoka, *Langmuir* **2006**, *22*, 4403
- ⁷⁴ H. Saito, Y. Takeoka, M. Watanabe, *Chem. Comm.* **2003**, 2126
- ⁷⁵ Y. Takeoka, M. Watanabe, *Adv. Mater.* **2003**, *15*, 199
- ⁷⁶ Y. Takeoka, M. Watanabe, R. Yoshida, *J. Am. Chem. Soc.* **2003**, *125*, 13320
- ⁷⁷ Y. Iwayama, J. Yamanaka, Y. Takiguchi, M. Takasaka, K. Ito, T. Shinohara, T. Sawada, M. . Yonese, *Langmuir* **2003**, *19*, 977
- ⁷⁸ J. R. Lawrence, G. H. Shim, P. Jiang, M. G. Han, Y. Ying, S. H. Foulger, *Adv. Mater.* **2005**, *17*, 2344
- ⁷⁹ J. Xia, Y. Ying, S. H. Foulger, *Adv. Mater.* **2005**, *17*, 2463
- ⁸⁰ K. Lee, S. A. Asher, *J. Am. Chem. Soc.* **2000**, *122*, 9534
- ⁸¹ M. M. W. Muscatello, S. A. Asher, *Adv. Funct. Mater.* **2008**, *18*, 1186
- ⁸² Y.-J. Lee, P. V. Braun, *Adv. Mater.* **2003**, *15*, 563
- ⁸³ J. Wang, Y. Han, *Langmuir* **2009**, *25*, 1855
- ⁸⁴ K. Ueno, K. Matsubara, M. Watanabe, Y. Takeoka, *Adv. Mater.* **2007**, *19*, 2807
- ⁸⁵ S. A. Asher, V. L. Alexeev, A.V. Goponenko, A. C. Sharma, I. K. Lednev, C. S. Wilcox, D. N. Finegold, *J. Am. Chem. Soc.* **2003**, *125*, 3322
- ⁸⁶ Y.-J. Lee, S. A. Pruzinsky, P. V. Braun, *Langmuir* **2004**, *20*, 3096
- ⁸⁷ D. Nakayama, Y. Takeoka, M. Watanabe, K. Kataoka, *Angew. Chem. Int. Ed.* **2003**, *42*, 4197
- ⁸⁸ A. C. Sharma, T. Jana, R. Kesavamoorthy, L. Shi, M. A. Virji, D. N. Finegold, S. A. Asher, *J. Am. Chem. Soc.* **2004**, *126*, 2971
- ⁸⁹ M. Kamenjicki, I. K. Lednev, A. Mikhonin, R. Kesavamoorthy, S. A. Asher, *Adv. Funct. Mater.* **2003**, *13*, 774
- ⁹⁰ K. Matsubara, M. Watanabe, Y. Takeoka, *Angew. Chem. Int. Ed.* **2007**, *46*, 1688
- ⁹¹ M. Kamenjicki, I. K. Lednev, S. A. Asher, *Adv. Funct. Mater.* **2005**, *15*, 1401
- ⁹² R. A. Barry, P. Wiltzius, *Langmuir* **2006**, *22*, 1369
- ⁹³ Y. Takeoka, M. Watanabe, *Langmuir* **2003**, *19*, 9554

-
- ⁹⁴ Y. Takeoka, M. Watanabe, *Langmuir* **2003**, *19*, 9104
- ⁹⁵ Y. Takeoka, T. Seki, *Langmuir* **2006**, *22*, 10223
- ⁹⁶ A. Toyotama, T. Kanai, T. Sawada, J. Yamanaka, K. Ito, K. Kitamura, *Langmuir* **2005**, *21*, 10268
- ⁹⁷ X. Xu, A. V. Goponenko, S. A. Asher, *J. Am. Chem. Soc.* **2008**, *130*, 3113
- ⁹⁸ J. Wang, Y. Cao, Y. Feng, F. Yin, J. Gao, *Adv. Mater.* **2007**, *19*, 3865
- ⁹⁹ P. Jiang, D.W. Smith Jr., J. M. Ballato, S. H. Foulger, *Adv. Mater.* **2005**, *17*, 179
- ¹⁰⁰ A. C. Arsenault, H. Miguez, V. Kitaev, G. A. Ozin, I. Manners, *Adv. Mater.* **2003**, *15*, 503
- ¹⁰¹ A. C. Arsenault, D. P. Puzzo, I. Manners, G. A. Ozin, *Nature Photonics* **2007**, *1*, 468.
- ¹⁰² D. P. Puzzo, A. C. Arsenault, I. Manners, G. A. Ozin, *Angew. Chem. Int. Ed.* **2009**, *48*, 943
- ¹⁰³ A. Arsenault, H. Miguez, I. Manners, G. A. Ozin, *U.S. Patent* 7364673, April 29, **2008**
- ¹⁰⁴ J. M. Jethmalani, W. T. Ford, *Chem. Mater.* **1996**, *8*, 2138
- ¹⁰⁵ J. M. Jethmalani, W. T. Ford, G. Beaucage, *Langmuir* **1997**, *13*, 3338
- ¹⁰⁶ J. M. Jethmalani, H. B. Sunkara, W. T. Ford, S. L. Willoughby, B. J. Ackerson, *Langmuir* **1997**, *13*, 2633
- ¹⁰⁷ S. H. Foulger, P. Jiang, A. C. Lattam, D. W. Smith, J. Ballato, *Langmuir* **2001**, *17*, 6023
- ¹⁰⁸ S. H. Foulger, P. Jiang, Y. Ying, A. C. Lattam, D. W. Smith Jr., J. Ballato, *Adv. Mater.* **2001**, *13*, 1898
- ¹⁰⁹ S. H. Foulger, P. Jiang, A. C. Lattam, D. W. Smith Jr., J. Ballato, D. E. Dausch, S. Grego, B. R. Stoner, *Adv. Mater.* **2003**, *15*, 685
- ¹¹⁰ K. Sumioka, H. Kayashima, T. Tszuzui, *Adv. Mater.* **2002**, *14*, 1284
- ¹¹¹ H. Fudouzi, Y. Xia, *Adv. Mater.* **2003**, *15*, 892
- ¹¹² H. Fudouzi, Y. Xia, *Langmuir* **2003**, *19*, 9653
- ¹¹³ H. Fudouzi, T. Sawada, *Langmuir* **2006**, *22*, 1365
- ¹¹⁴ A. C. Arsenault, T. J. Clark, G. von Freymann, L. Cademartiri, R. Sapienza, J. Bertolotti, E. Vekris, S. Wong, V. Kitaev, I. Manners, R. Z. Wang, S. John, D. Wiersma, G. A. Ozin, *Nature Materials* **2006**, *5*, 179
- ¹¹⁵ W. Wohlleben, F. W. Bartels, S. Altmann, R. J. Leyrer, *Langmuir* **2007**, *23*, 2961
- ¹¹⁶ O. L. J. Pursiainen, J. J. Baumberg, K. Ryan, J. Bauer, H. Winkler, B. Viel, T. Ruhl, *Appl. Phys. Lett.* **2005**, *87*, 101902
- ¹¹⁷ B. Viel, T. Ruhl, G. P. Hellmann, *Chem Mater.* **2007**, *19*, 5673
- ¹¹⁸ O. L. J. Pursiainen, J. J. Baumberg, H. Winkler, B. Viel, P. Spahn, T. Ruhl, *Optics Express* **2007**, *15*, 9553
- ¹¹⁹ A. Okabe, T. Fukushima, K. Ariga, T. Aida, *Angew. Chem. Int. Ed.* **2002**, *41*, 3414
- ¹²⁰ J. Yoon, W. Lee, E. L. Thomas, *Macromolecules* **2008**, *41*, 4582

-
- ¹²¹ C. Kang, E. Kim, H. Baek, K. Hwang, D. Kwak, Y. Kang, E. L. Thomas, *J. Am. Chem. Soc.* **2009**, *131*, 7538
- ¹²² S. Y. Choi, M. Mamak, G. von Freymann, N. Chopra, G. A. Ozin, *Nano Lett.* **2006**, *6*, 2456
- ¹²³ B. V. Loshch, G. A. Ozin, *Adv. Mater.* **2008**, *20*, 4079
- ¹²⁴ P. El-Kallassi, R. Ferrini, L. Zuppiroli, N. Le Thomas, R. Houdré, A. Berrier, S. Anand, A. Talneau, *J. Opt. Soc. Am. B.* **2007**, *24*, 2165
- ¹²⁵ B. Gauvreau, N. Guo, K. Schicker, K. Stoeffler, F. Boismenu, A. Ajji, R. Wingfield, C. Dubois, M. Skorobogatiy, *Optics Express* **2008**, *16*, 15677
- ¹²⁶ W. Park, J.-B. Lee, *OPN* **2009**, January, 40
- ¹²⁷ J. B. Pendry, *Phys. Rev. Lett.* **2000**, *85*, 3966
- ¹²⁸ S. Noda, M. Fujita, T. Asano, *Nature Photonics*, **2007**, *1*, 449
- ¹²⁹ T. Prasad, V. Colvin, D. Mittleman, *Phys. Rev. B* **2003**, *67*, 165103
- ¹³⁰ Stöber W; Fink A. Controlled growth of monodisperse silica spheres in the micron size range, *J. of Colloid and Interface Science* **1968**, *26*, 62
- ¹³¹ Xia Y.; Gates B.; Yin Y.; Lu Y. Monodispersed colloidal spheres: old materials with new applications *Adv. Mater.* **2000**, *12*, 693
- ¹³² Patton T. C. in *Pigment Handbook Volume I*, John Wiley & sons Inc. 1973
- ¹³³ Church A. H. in *The chemistry of paints and painting* Cap XIX pag 239, Book available on line http://books.google.com/books?id=N0MTAAAYAAJ&dq=indian+ink+chemistry&source=gbs_navlinks_s
- ¹³⁴ <http://refractiveindex.info/?group=PLASTICS&material=PMMA>
- ¹³⁵ <http://refractiveindex.info/?group=CRYSTALS&material=SiO2>
- ¹³⁶ McGrath J. G.; Bock R. D.; Cathcart J. M.; Lyon L. A. Self-assembly of “paint-on” colloidal crystals using poly (styrene-co-N-isopropylacrylamide) spheres, *Chem. Mater.* **2007**, *19*, 1584
- ¹³⁷ Takeoka Y.; Honda M.; Seki T.; Ishii M.; Nakamura H. *Applied Materials & Interfaces* **2009**, *1*, 982
- ¹³⁸ Balestreri A.; Andreani L. C. Optical properties and diffraction effects in opal photonic crystals *Phys. Rev. E* **2006**, *74*, 036603
- ¹³⁹ Vlasov Y. A.; Astratov V. N.; Baryshev A. V.; Kaplyanskii A. A.; Karimov O.Z.; Limonov M. F. Manifestation of intrinsic defects in optical properties of self organized opal photonic crystals *Phys. Rev. E* **2000**, *61*, 5784
- ¹⁴⁰ Astratov V. N.; Adawi A. M.; Fricker S.; Skolnick M. S.; Whittaker D. M.; Pusey P. N. Interplay of order and disorder in the optical properties of opal photonic crystals *Phys. Rev. B* **2002**, *66*, 165215

-
- ¹⁴¹ Koenderink A. F.; Lagendijk A.; Vos W. L. Optical extinction due to intrinsic structural variations of photonic crystals *Phys. Rev. B* **2005**, 72, 153102
- ¹⁴² Sigalas M.M.; Soukoulis C. M.; Chan C. T.; Ho K. M. Electromagnetic –wave propagation through dispersive and absorptive photonic-band-gap materials *Phys. Rev. B* **1994**, 49, 11080
- ¹⁴³ Dorado L. A.; Depine R. A. Modeling of disorder effects and optical extinction in three dimensional photonic crystals *Phys. Rev. B* **2009**, 79, 045124
- ¹⁴⁴ H. C. van de Hulst in *Light scattering by small particles* New York, Dover, **1981**
- ¹⁴⁵ Pursiainen O. L. J.; Baumberg J. J.; Winkler H.; Viel B.; Spahn P. ; Ruhl T. Nanoparticle-tuned structural color from polymer opals *Optics Express* **2007**, 15, 9553
- ¹⁴⁶ Wang X. H.; Akahane T.; Orikasa H.; Kyotani T. Brilliant and tunable color of carbon-coated thin anodicaluminium oxide films *Appl. Phys. Lett.* **2007**, 91, 011908
- ¹⁴⁷ Gutcho M. H. (ed.) in *Inorganic Pigments Manufacturing Processes* Noyes Data Co. New Jersey, USA **1980**; Cap 5, pag. 187
- ¹⁴⁸ Bohren C. F.; Huffmann D. R. in *Absorption and scattering of light by small particles*. Germany, Wiley VCH, **2004**
- ¹⁴⁹ Ishimaru A. in *Wave Propagation and Scattering in Random Media*, IEEE Press Oxford University Press USA, **1997**
- ¹⁵⁰ Vlasov Y. A.; Kaliteevski M. A.; Nicolaev V.V. Different regimes of light localization in a disordered photonic crystal *Phys. Rev. B* **1999**, 60, 1555
- ¹⁵¹ Koenderink A. F.; Lagendijk A.; Vos W. L. Optical extinction due to intrinsic structural variations of photonic crystals *Phys. Rev. B* **2005**, 72, 153102
- ¹⁵² Liu L.; Li P.; Asher S. A.; Fortuitously superimposed lattice plane secondary diffraction from crystalline colloidal arrays *J. Am. Chem Soc.* **1997**, 119, 2729
- ¹⁵³ Tikhonov A.; Coalson R. D.; Asher S. A. Light diffraction from colloidal crystals with low dielectric constant modulation: simulations using single scattering theory *Phy. Rev. B* **2008**, 77, 235404
- ¹⁵⁴ García P. D.; Sapienza R.; Blanco A.; López C. Photonic glass: a novel material for light *Adv. Mater.* **2007**, 19, 2597
- ¹⁵⁵ García P. D.; Sapienza R.; Bertolotti J.; Martin M. D.; Blanco A.; Altube A.; Viña L.; Wiersma D. S.; López C. Resonant light transport through Mie modes in photonic glasses *Phys. Rev. A* **2008**, 78, 023823